

MASTERARBEIT / MASTER'S THESIS

Titel der Masterarbeit / Title of the Master's Thesis

„Microglial nodules and their potential role in brain
inflammation“

verfasst von / submitted by

Denise Gessl, BSc

angestrebter akademischer Grad / in partial fulfilment of the requirements for the degree of
Master of Science (MSc)

Wien, 2018 / Vienna 2018

Studienkennzahl lt. Studienblatt /
degree programme code as it appears on
the student record sheet:

A 066 834

Studienrichtung lt. Studienblatt /
degree programme as it appears on
the student record sheet:

Masterstudium Molekulare Biologie

Betreut von / Supervisor:

Ao.Univ.Prof. Dr. Jan Bauer

Statement of Authorship

I hereby declare that this master's thesis is entirely authored by myself and I have not used any other literature sources than those listed in the references. Furthermore, I state not to submit my thesis to any institution to receive another degree. I endeavoured to find all owners of the image rights and to obtain their consent to the use of the images in this work. Nevertheless, if a copyright infringement becomes known, I request for report to me.

Denise Gessl

Wien, 01.02.2018

Acknowledgements

First of all, I want to thank Jan Bauer for giving me the opportunity to work in his lab and on this exciting project. I am grateful for his support and all the knowledge he shared with me throughout the project.

I want to express my gratitude to Anna Tröscher, MSc, for introducing me to all the important techniques I needed and her helpfulness during my thesis. You showed me all the important things I have to know and always had an open ear for discussing problems.

Further, I like to thank Ulrike Köck, Marianne Leißer and Angela Kury for sharing their knowledge in histochemistry with me and their constant technical support during my experiments. My thanks go also to Markus Jeitler of the Core facilities of the Medical University, for performing RNA quality and quantity measurements.

Thanks to my colleagues of the Center for Brain research, it was a great time with you and I had a lot of fun, especially in the lunch breaks.

Lastly, I want to thank my parents, my boyfriend and my friends. My boyfriend receives special thanks, as he always cheered me up in hard times and was there for me and encouraged me whenever I needed it. Thanks to my parents for being always there for me and supporting me throughout my life.

Abstract

Rasmussen encephalitis (RE) is a rare, progressive neurological disease that is characterized by unilateral drug-resistant seizures, hemiparesis and cognitive decline. One of the histopathological hallmarks are microglial nodules, which are common findings in inflammatory diseases of the central nervous system (CNS). In RE, they are mainly found in the cortex and are considered as one of the earliest pathologic abnormalities. However, their role in the inflammatory reactions is not clear. Recently, multiprotein complexes termed inflammasomes have received growing attention. Inflammasomes are expressed in the CNS and can be activated by various substances.

To gain better insight into the inflammatory pathways, we studied interleukin-18 (IL-18) and caspase 1, as components of the inflammasome, in RE. IL-18 is a pro-inflammatory cytokine that needs to be cleaved into its active form by caspase 1. We analyzed the gene expression of these components by quantitative real-time polymerase chain reaction (qPCR) and performed immunohistochemistry (IHC) and quantification of IL-18 positive cells. Furthermore, we performed IHC to investigate the communication of microglia with (cytotoxic) T cells and for P-Stat1, as a surrogate marker for IFN signaling in microglial nodules.

The qPCR results revealed that gene expression of IL-18 is significantly increased in the early stage of RE compared to the controls. Expression of caspase 1 showed a significant increase in the intermediate stage. Results obtained from the quantification of IL-18 positive cells confirmed our findings from qPCR. Besides, we noted IL-18 and caspase 1 positive small nodules in stage 0. The evaluation of double stainings for microglia and (cytotoxic) T cells showed that nodules consisting of 3-4 microglial cells rarely contain T cells, while large nodules (>10 cells) always exhibited T cell infiltration. Phospho-Stat1 was observed in microglial cells and neurons.

This work presents the upregulation of IL-18 and caspase 1 and the presence in microglial nodules of early stage RE. Based on our findings, we suggest that T cells or IFNs do not trigger the earliest microglial inflammasome activation, but are involved in further activation of microglial cells in nodules. Further studies are needed to investigate the inflammatory signaling cascades that lead to microglial production of cytokines and chemokines and thereby attract cytotoxicity mediating T cells.

Zusammenfassung

Rasmussen Enzephalitis (RE) ist eine seltene, progressive neurologische Erkrankung, die durch unilaterale medikamentenresistente epileptische Anfälle, Hemiparese und kognitiven Verfall charakterisiert ist. Zu den wichtigsten histopathologischen Merkmalen zählen Mikroglia Knötchen. Die Knötchen sind ein Kennzeichen in entzündlichen Erkrankungen des Zentralnervensystems (ZNS). In RE treten diese vermehrt im Cortex auf und werden als eine der frühesten pathologischen Veränderung betrachtet. Ihre Rolle in den Entzündungsprozessen ist jedoch unklar. In letzter Zeit wurde den multiprotein Komplexen, die als Inflammasome bezeichnet werden, zunehmend Beachtung geschenkt. Inflammasome werden im ZNS exprimiert und können durch eine große Auswahl an Substanzen aktiviert werden.

Um ein besseres Verständnis für die entzündlichen Signalwege zu bekommen, untersuchten wir die Inflammasom Komponenten Interleukin-18 (IL-18) und Caspase 1 in RE. IL-18 ist ein proinflammatorisches Zytokin, das durch Caspase 1 in seine aktive Form gespalten wird. Wir analysierten die Genexpression von diesen Komponenten mittels qPCR und quantifizierten IL-18 positive Zellen durch Immunohistologie. Darüberhinaus untersuchten wir mit Hilfe von immunohistologischen Färbungen die Kommunikation zwischen Mikroglia und (zytotoxischen) T-Zellen, sowie die Anwesenheit von Phospho-Stat1 in Knötchen.

Die qPCR Analysen enthüllten, dass die Genexpression von IL-18 im frühen RE Stadium deutlich gesteigert ist im Vergleich zu den Kontrollen. Die Expression von Caspase 1 war im intermediären Stadium deutlich erhöht. Diese Ergebnisse wurden mit immunohistochemischer Quantifizierung von IL-18 bestätigt. Zudem fanden wir IL-18 und Caspase 1 positive kleine Knötchen im frühesten Stadium. Die Auswertung von Doppelmarkierungen zeigte, dass in Knötchen bestehend aus 3-4 Mikrogliazellen kaum T-Zellen vorhanden waren, während große Knötchen stets T-Zell-Infiltration aufwiesen. Phospho-Stat1, ein Protein das in der Interferon-Signalkaskade beteiligt ist, konnte in Mikrogliazellen und Neuronen detektiert werden.

Diese Arbeit zeigt die Hochregulierung von IL-18 und Caspase 1 und deren Präsenz in Mikroglia Knötchen im frühen Stadium von RE. Diese Ergebnisse führen zu der Hypothese, dass weder T-Zellen noch Interferone die früheste Inflammation Aktivierung in Mikroglia provozieren. Weitere Studien sind notwendig um die entzündlichen Signalkaskaden die zur Produktion von Zytokinen und Chemokinen in Mikroglia führen und dadurch zytotoxische T-Zellen anziehen.

Table of Contents

1	Introduction	1
1.1	Rasmussen encephalitis	1
1.2	Viral encephalitis	4
1.3	Mesial temporal lobe epilepsy	6
1.4	Inflammation	6
1.4.1	Inflammation in the central nervous system	7
1.5	Neuroinflammation and epilepsy	8
1.6	Microglial nodules – common feature among inflammatory CNS diseases	11
1.7	The Inflammasome	12
1.8	Interleukin-18 and its role in neuroinflammation	15
1.9	Objectives of the thesis	16
2	Materials and Methods	18
2.1	Human Study Samples	18
2.2	Deparaffinization	18
2.2.1	Materials	18
2.2.2	Method	18
2.3	Hematoxylin-Eosin (HE) staining	19
2.3.1	Materials	19
2.3.2	Method	19
2.4	Immunohistochemistry	20
2.4.1	Single staining for light microscopy	20
2.4.2	Double stainings for light microscopy	20
2.5	Confocal Laser Fluorescence Microscopy	25
2.5.1	Materials	25
2.5.2	Method	27
2.6	RNA Isolation	27
2.6.1	Materials	27
2.6.2	Method	28
2.6.3	RNA Quality Measurement	31
2.7	Reverse Transcription PCR	31
2.7.1	Materials	31
2.7.2	Method	31
2.8	Quantitative Real-Time PCR	32
2.8.1	Materials	32
2.8.2	Method	32
2.9	Statistical Analysis	34
3	Results	36
3.1	RNA quality measurement	36
3.2	Analysis of Interleukin-18 and Caspase 1 mRNA levels in Rasmussen encephalitis and Mesial temporal lobe epilepsy	37
3.2.1	Elevated expression of Caspase 1 in intermediate stage of RE	38
3.2.2	Interleukin-18 expression increased in early stage of RE	38
3.3	Qualitative and quantitative immunohistochemical evaluation	39
3.3.1	Presence of Interleukin-18 in Rasmussen encephalitis and Mesial temporal lobe epilepsy	39
3.3.2	Microglial nodules in Rasmussen encephalitis and viral encephalitis	42
4	Discussion	48

5	List of Abbreviations.....	52
6	References	54
7	Appendix	60
7.1	Clinical data of included patients	60

1 Introduction

Epilepsy is a chronic brain disorder and one of the most common neurological conditions, affecting about 50 million people in the world (Vezzani et al., 2011). It is characterized by recurrent, unprovoked epileptic seizures as a result of hyperexcitability, atypical and synchronized firing of groups of neurons along with cognitive and emotional malfunctions (Matin et al., 2015). Despite of the many antiepileptic drugs (AEDs) that are available for treatment, 30% of the patients do not respond to therapy and continue to suffer from seizures (Perucca et al., 2007). While AEDs target mostly symptomatic relief, they do not take effect on the underlying pathology of the disease. It is therefore all the more important to reveal the etiology of epilepsy (Matin et al., 2015; Vezzani et al., 2011). Epileptic seizures in adults develop often in response to structural changes after brain injuries, stroke or tumors (Pitkanen et al., 2007; Scharfman, 2007). In children, infections, fever and head trauma are common causes of epileptic seizures (Cowan, 2002).

1.1 Rasmussen encephalitis

In the 1950s, neurosurgeon Theodore Rasmussen was the first to describe Rasmussen encephalitis (RE) as seizures due to chronic localized encephalitis (Rasmussen et al., 1958). Mainly children and young adults are affected by this rare disease. It is a progressive, neurological disorder characterized by pharmaco-resistant unilateral epileptic seizures, cognitive deterioration, accompanied by cerebral hemiatrophy, and progressive hemiparesis (Varadkar et al., 2014). According to a German study, the estimated incidence is 2.4 new cases per year per 10 million people aged 18 and younger (Bien et al., 2013).

Magnetic resonance imaging (MRI) is becoming a valuable tool for diagnosis and follow-up of RE (Bien et al., 2002b). Patients often present a hyperintense T2 signal in cortical or subcortical regions with heterogeneous distribution. The area around the Sylvian fissure is a preferred site for volume loss and signal change (Figure 1) (Varadkar et al., 2014)

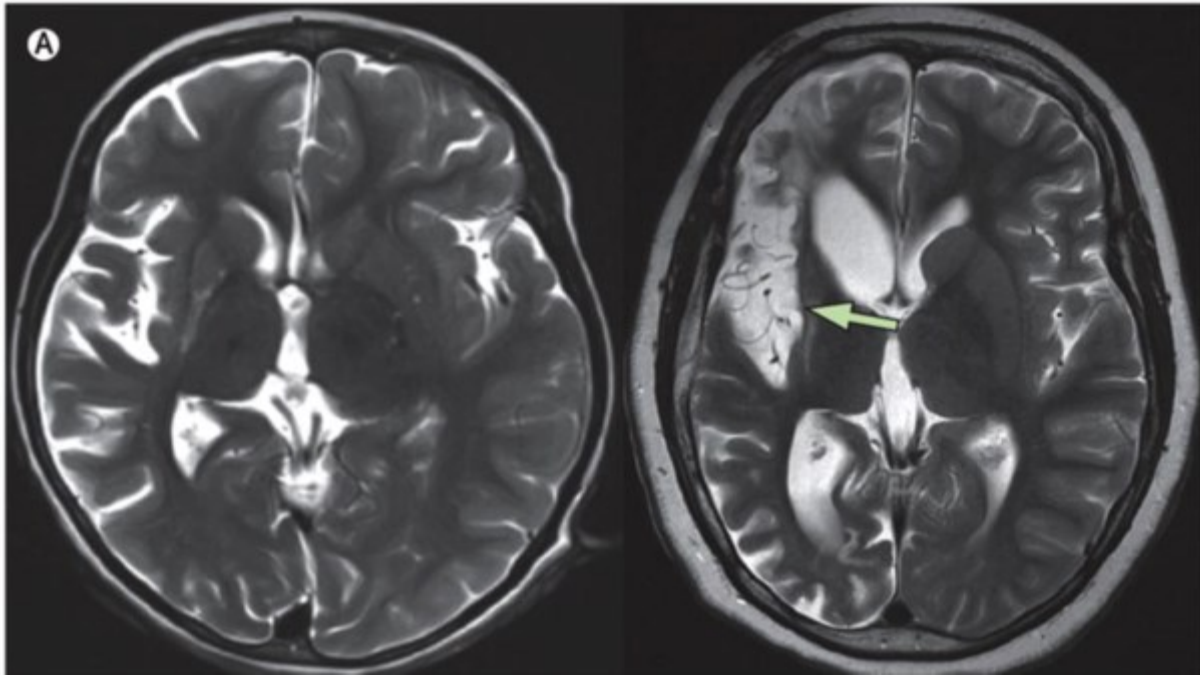


Figure 1. MRI brain scan of a child with RE. From left to right: The scan shows progressive atrophy of the right hemisphere with high signal and basal ganglia loss over a period of 1 year. The arrow on the right picture indicates the affected area near the right Sylvian fissure (Varadkar et al., 2014)

The treatment of RE pursues a two-fold aim: the prevention of seizures and the cessation of progression of neurological decline. Since the seizures often are resistant to medical treatment, radical neurosurgical interventions remain the only option. Hemispherectomy is the most promising technique for achieving seizure freedom, but is associated with major neurological deficits. Nowadays, the affected hemisphere is only functionally disconnected from the other one and not entirely resected (Bien et al., 2005). The advantage of this technique is that there is a lower incidence of complications in comparison to the full resection of the hemisphere (Jonas et al., 2004). However, consequences after hemispherectomy have to be expected, such as spastic hemiplegia and hemianopia (Bien et al., 2005)

In terms of histopathology, typical features of the affected hemisphere are cortical inflammation, formation of microglia nodules, infiltration of T lymphocytes, astrogliosis, neuronophagia and neuronal loss. Microglial nodules are common findings in inflammatory CNS diseases and can already occur in the early stage of RE (Pardo et al., 2004; Varadkar et al., 2014). Table 1 gives an overview of the histopathological changes in the 5 different stages of Rasmussen encephalitis (Pardo et al., 2004).

Stages	Stage 0	Stage 1	Stage 2	Stage 3	Stage 4
Definition	Normal cortex	Early stage	Intermediate stage	Late stage	End stage
Cerebral cortex	Normal	Mild focal inflammation and gliosis	Panlaminar cortical inflammation and gliosis	Panlaminar cortical degeneration and gliosis	Panlaminar cortical cavitation and/or gliosis
Neuronal loss	Absent	Minimal, focal	Moderate to severe, multifocal	Severe, panlaminar	Severe, rare neurons
Astrogliosis	Absent	Mild to moderate, focal	Marked, frequently panlaminar, gemistocytes	Marked, panlaminar, gemistocytes	Variable
Microglial activation	Absent	Mild to moderate, focal	Marked, panlaminar	Variable	Variable
T-cell infiltration	Absent	Mild to moderate, few T-lymphocyte clusters and perivascular cuffs	Marked, panlaminar or multifocal, frequent perivascular cuffs	Minimal	Rare

Table 1. Stages of cortical pathology in Rasmussen encephalitis (Pardo et al., 2004).

In the course of disease an increase of T lymphocyte infiltration, astrogliosis and microglial activation reactions in the cortex are noted. During the early stage there is only little evidence of neuronal loss, whereas in the intermediate stage neuronal injury can be observed. Besides, the intermediate stage shows a significant rise in T cell infiltration and cortical inflammation and gliosis progress from a focal to a panlaminar distribution. The late stage is defined by the depletion of neurons in the cortical layers and severe atrophy, but the inflammatory process subsides and only a few T lymphocyte clusters are seen. The end stage is characterized by massive destruction of the cerebral cortex with extensive neuronal loss and cavitation or vacuolation. In such regions remaining astrogliosis can be present, while inflammatory changes are scarce or even absent (Bien et al., 2002b; Pardo et al., 2004).

The cause of Rasmussen encephalitis still remains elusive and numerous pathological mechanisms have been suggested. It is most likely that the inflammation of the brain is triggered by an antigen that could be either an infectious agent or autoimmune (Takei et al., 2010; Varadkar et al., 2014).

Cytotoxic T cells play a pivotal role in RE, because they attack neurons and astrocytes which further leads to neuronal and astrocyte loss (Bauer et al., 2007; Bien et al., 2002a). The presence of lymphocyte infiltration and microglial nodules in RE appears similar to the infection with a particular flavivirus (Bien et al., 2005). Furthermore, researchers hypothesized that the T cells recognize virus-infected cells and examined tissue samples from RE patients for the presence of various viruses, including cytomegalovirus (CMV), herpes simplex virus (HSV), Epstein-Barr virus (EBV) and enterovirus. Nevertheless, none of these studies was able to confirm a

causal relationship between RE and a particular virus (Friedman et al., 1977; Jay et al., 1995; Power et al., 1990; Varadkar et al., 2014; Walter and Renella, 1989).

Besides the T cell mediated response, microglial activation is another neuropathological mechanism that is involved in central nervous system (CNS) degeneration (Varadkar et al., 2014). Banati and colleagues discovered widespread microglial activation in the affected hemisphere of patients (Banati et al., 1999). However, further studies are needed to completely clarify the pathogenic role of microglia in RE. Taken together, the underlying principles of disease development are still unknown.

1.2 Viral encephalitis

Infections with viruses are widespread and are often rapidly cleared by the immune system. Some viruses can enter the brain by different routes and cause serious damage such as the formation of acute encephalitis (Steiner et al., 2005). Prominent viruses that can cause encephalitis are herpes simplex virus (HSV), cytomegalovirus (CMV), tick-borne encephalitis virus (TBEV), rabies virus, Epstein-Barr virus, John Cunningham virus (JCV) and human immunodeficiency virus (HIV) (van den Pol, 2006). Typical symptoms are fever, headache, disturbed consciousness and sometimes seizures and focal neurological abnormalities. Medical treatment should be started early in the course of encephalitis to avoid permanent damage and reduce the mortality (Steiner et al., 2005).

Infections with CMV and JCV are often found in patients with an immunosuppression, such as patients suffering from AIDS, where the virus gets reactivated after a latent period (Quinnan et al., 1984).

JCV is the cause for progressive multifocal leukoencephalopathy (PML), a deadly opportunistic demyelinating disease of the CNS (Quinnan et al., 1984; Wuthrich et al., 2006). It is characterized by infected oligodendrocytes that are found around demyelinating lesions of the white matter, bizarre-looking astrocytes in burnt out lesions and an inflammatory response with lymphocytic infiltration (Berger, 2007; Richardson and Webster, 1983). Unfortunately, there is no cure for PML yet, but researchers are performing clinical trials with various agents that may be potential candidates for harming the virus. Currently, the most important approach is the optimal reconstitution of the immune system to control the virus and prolong the

survival of patients (Pavlovic et al., 2015; Weissert, 2011). In recent years, the occurrence of PML is once again on the rise, due to the introduction of immunosuppressive drugs for patients suffering from autoimmune disorders or cancer (Laukoter et al., 2017).

The herpesvirus family is highly prevalent in nature and is able to establish a lifelong latency within the host. One member of interest is the herpes simplex virus (HSV) that can cause CNS manifestations. Herpesviruses inducing CNS infections are a significant cause for morbidity, mortality and especially long-term neurological complications (James et al., 2009). Encephalitis caused by HSV is regarded as one of the most common causes of sporadic, fatal encephalitis (Olson et al., 1967) and mainly occurs in individuals 6 months to 20 years of age or older than 50 years (Whitley et al., 1982). In 70% of all cases the herpes simplex encephalitis (HSE) is caused by a recurrent infection, in the remaining 30% HSE arises as primary infection (Nahmias et al., 1982). The mortality rate is about 70% without any treatment, and of the patients that survive, remarkable neurologic morbidity occurs in approximately 97% (Kimberlin, 2007). HSV infects neurons, astrocytes and oligodendrocytes, but prefers to attack neurons and resides there until it gets fully reactivated again (Bertke et al., 2009). Histological characteristics for HSE are necrotic and hemorrhagic foci in the temporal or frontal lobes, microglial activation and infiltration of leukocytes (Conrady et al., 2010; Kleinschmidt-DeMasters et al., 2001).

Cytomegalovirus belongs to the family of herpesviruses and is one of the most common infections worldwide. CMV infections often occur in the first 2 decades of life, but can also happen congenitally, perinatally, intrauterine or postnatally. The pathogenesis with CNS involvement starts with the virus infecting endothelial cells in the brain, then spreading to astrocytes near the epithelium and further invading neurons. Periventricular inflammation, microglial nodules and parenchymal focal necrotic lesions are histopathological characteristics (Arribas et al., 1996; James et al., 2009).

Examination of brain tissue samples from viral encephalitis patients showed numerous microglial nodules spread throughout the brain. (Imaizumi et al., 2005).

Samples from HSV, CMV, PML and TBEV patients were used for studying microglial nodules in this project.

1.3 Mesial temporal lobe epilepsy

Mesial temporal lobe epilepsy (MTLE) is one of the two main types of temporal lobe epilepsy (TLE), originating in the hippocampus, parahippocampal gyrus and amygdala (Thom, 2014). The causes of the seizures include mesial temporal sclerosis, encephalitis, hypoxic brain injury and TBI (Davies et al., 1995; Epstein et al., 2012; Vespa et al., 2010). Mesial temporal sclerosis, also known as hippocampal sclerosis (HS), is a prominent hallmark in MTLE and other epileptic disorders.

Histological hallmarks include the loss of pyramidal neurons, granule cell dispersion and gliosis especially in the Cornu Ammonis area 1 (CA1) and subiculum of the hippocampus (Prayson, 2010).

The etiology of HS is still debated and may be multifactorial (Thom, 2014). There is a strong link between prolonged febrile seizures in early childhood and hippocampal sclerosis (Lewis et al., 2014). Many patients suffer an initial insult or injury in early infancy, followed by a latent period without any signs of seizures and ultimately results in recurrent seizures (Scharfman, 2007).

Furthermore, HS has a conflicting interest regarding epilepsy. On one hand, the hippocampus is highly susceptible to injury by seizures and other insults. On the other hand, the injured hippocampus is also the cause of epileptic seizures (Thom, 2014; Walker, 2015).

1.4 Inflammation

Acute inflammation arises often from harmful stimuli such as infection, tissue injuries or growing tumors and is destined to fight invading pathogens. In response to these stimuli, the immune system initiates a cascade of pro-inflammatory as well as anti-inflammatory mediators and other immunomodulating agents. Inflammation is indicated by immune cells in tissues or circulating in the blood that produce an array of inflammatory molecules (Vezzani et al., 2011). The main goal is the promotion of tissue repair and recovery of homeostasis (Antonelli and Kushner, 2017).

The first line of defense is the innate immune system, which responds with inflammation against intruders (Becker, 2006). Interleukins (ILs), interferons (IFNs)

and tumor necrosis factors (TNFs) are members of the cytokine family and are inflammatory mediators that have a crucial function in the transition from innate to adaptive immunity (Nguyen et al., 2002).

IFNs have numerous biological effects on the target cells, namely antiviral, anti-proliferative and immunomodulatory activities. IFNs can be grouped in 2 main classes: Type I and type II IFNs. The members of the type I family are IFN α , IFN β and IFN ω , while the type II family consists only of IFN γ (González-Navajas et al., 2012). Almost all cell types produce type I IFNs upon exposure to invading pathogens or damage-associated molecular patterns (DAMPs). In contrast, type II IFNs are primarily produced by T cells and natural killer cells. All type I IFNs bind to the same receptor (IFNAR), whereas IFN γ binds to a different receptor (IFNGR) (Pestka et al., 2004; Platanias and Fish, 1999). One of the most prominent pathways for IFN signaling is the Jak-Stat pathway. It involves the activation of tyrosine kinases from the Janus family (Jak) and tyrosine phosphorylation of Stat proteins (signal transducers and activators of transcription). The Jak1 and Tyk2 kinases are linked to the receptor subunits and get activated upon ligand binding. Subsequently, they phosphorylate the receptor subunits and recruit Stat proteins, which then also become phosphorylated, dimerize and can translocate to the nucleus and initiate the transcription of target genes (Platanias and Fish, 1999; Rawlings et al., 2004). IFN γ responses are mainly mediated by Stat1 homodimers, while Stat1/Stat2 heterodimers are responsible for IFN type I responses (Rauch et al., 2013).

1.4.1 Inflammation in the central nervous system

Although the CNS is seen as an immunoprivileged site, there is growing evidence that inflammatory and immune reactions can occur within the CNS in response to infectious agents or various CNS injuries, such as ischemic or excitotoxic damage, traumatic brain injury (TBI) or epileptic seizures (Vezzani and Granata, 2005). Neurons, astrocytes and microglia are associated with processes of the innate immunity that play a part in the onset of brain inflammation. Since microglia are the immune cells of the CNS, they are the first responders to even minor pathological changes in the brain. These macrophage-like cells become activated and are able to secrete cytokines that trigger an inflammatory response (Ousman and Kubes, 2012). This occurrence is called neuroinflammation and is provoked to protect the CNS (Cherry et al., 2014). However, protracted and uncontrolled inflammation contributes

to brain pathology and may lead to neuronal damage or even neuronal death (Heneka et al., 2014).

In healthy condition, the blood-brain barrier (BBB) shields the CNS from the unrestrained entry of blood-borne cells and molecules. Furthermore, the BBB plays a central role in the interaction between neural cells and peripheral immune cells (Vezzani et al., 2011). During systemic inflammation, the permeability of the BBB is altered directly by ruptured tight junctions, upregulated vesicular traffic and pathological astrocyte changes or indirectly by modifications of transporters, cytokines and cellular transmigration (Varatharaj and Galea, 2017). Indirect alterations of the permeability are implicated in the stimulation of passage of leukocytes across the BBB (Gloor et al., 2001). In contrast to the acute inflammatory state, chronic inflammation is characterized by the persistence of active inflammation and infiltration of mononuclear immune cells such as macrophages, monocytes, lymphocytes and plasma cells. These cells or the secreted cytokines contribute to the destruction of the tissue and fibrosis in this pathological condition (Khansari et al., 2009). The production of chemokines by microglia recruits more immune cells to the inflamed area in the brain parenchyma (Ousman and Kubes, 2012).

1.5 Neuroinflammation and epilepsy

Over the past decade, research interest in the relationship between epilepsy and inflammation has increased remarkably. Emerging clinical and experimental evidences support the hypothesis that inflammatory activities in the brain might contribute to the pathophysiology of seizures and epilepsy. The initial findings arise from clinical evidence demonstrating that steroids and other anti-inflammatory drugs have anticonvulsant effects in some pharmaco-resistant epilepsies (Vezzani et al., 2011).

Moreover, resected brain tissue from patients suffering from refractory epilepsies, such as TLE and focal cortical dysplasia related epilepsy, presented high levels of pro-inflammatory mediators such as cytokines and noticeable cellular injury (Choi et al., 2009).

In recent years, there is strong evidence emerging that inflammation might be a consequence as well as a cause of epilepsy. It is possible that chronic inflammation might be intrinsic to some epilepsies, which are not associated with immunological

dysfunctions, rather than being a consequence of inflammatory or autoimmune processes. Experimental models have given more insight in the role of inflammation in epileptic disorders and the underlying mechanisms. For investigation whether seizures cause inflammation, researchers provoked recurrent short seizures or single prolonged seizures in adult rodents (Vezzani et al., 2011). These experiments revealed that the expression of pro-inflammatory mediators is notably elevated in brain regions of high seizure activity after seizure stimulation. Immunohistochemical examinations of rodent brain slices exposed that the production of IL-1 β , TNF- α and IL-6 is primarily upregulated in microglia and astrocytes, and the synthesis of the corresponding receptors is rapidly increased in microglia, astrocytes and neurons (Vezzani and Granata, 2005). The presence of brain inflammation might then endorse the recruitment of peripheral immune cells into the CNS. Neurons and glial cells express chemokines that direct T cells into the brain. In fact, a cascade of inflammatory events is induced in endothelial cells by seizures that results in an altered blood-brain barrier function. The upregulation of IL-1 β and its receptor, the complement system and adhesion molecules leads to a cerebrovascular inflammation involving seizure-activated perivascular glia that produce cytokines and prostaglandins (Ravizza et al., 2008; Vezzani et al., 2011).

Another important experimental approach deals with the idea that inflammation causes seizures. Evidence from rodent models suggests that brain inflammation supports neuronal hyperexcitability and seizures. Researchers already proved that inflammatory mediators like IL-1 β , IL-6 and TNF- α have an active role in seizure formation and exacerbation. Seizures trigger the production of pro-inflammatory molecules, which then influence seizure severity and recurrence (Figure 2) (Vezzani et al., 2011). Supplementary data points out that fever is the most common reason for seizures in children worldwide (Dube et al., 2007). The release of cytokines in the brain may contribute to the generation of febrile seizures and epileptogenesis afterwards (Dube et al., 2007; French et al., 1993). Ultimately, systemic injection of lipopolysaccharide (LPS) in a rat model lowers the seizures threshold and therefore enhances seizure susceptibility (Sayyah et al., 2003). LPS-induced modifications of the seizure threshold can be ascribed to the production of cytokines (e.g. IL-1 β and TNF) (Vezzani et al., 2011).

If inflammation indeed contributes to generation of epilepsy, the cycle of seizures triggering inflammation and inflammation aggravating seizures offers an important opportunity of treatment, by means of targeting components of this cascade (Edye et al., 2014). The presumed modes of action include suppressing inflammation, preventing hyperexcitability and inhibiting the release of endogenous proconvulsant mediators (Vezzani et al., 2011).

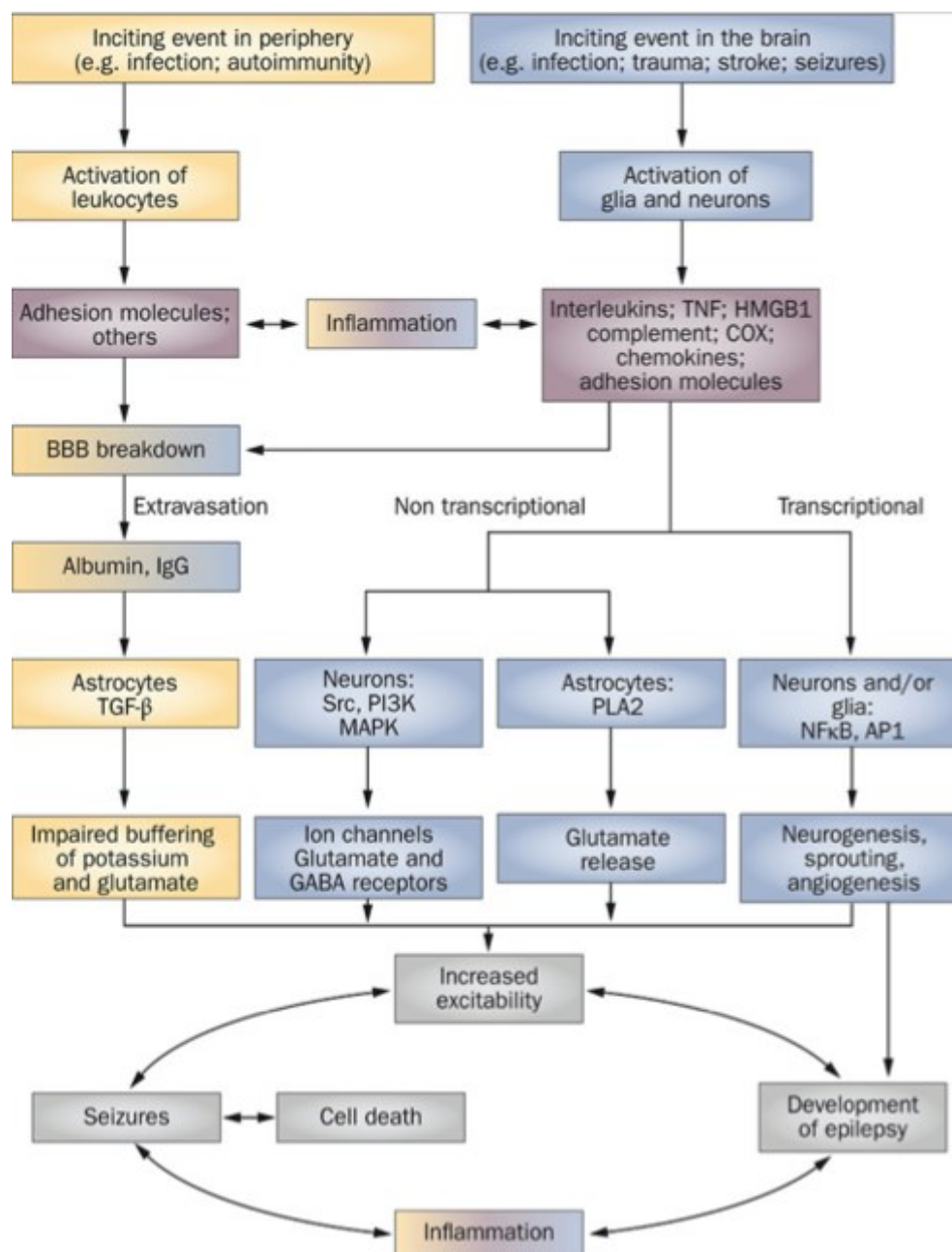


Figure 2. Pathophysiological cascade of inflammatory actions in epilepsy. The peripheral pathway is shown in yellow, the CNS pathway is depicted in blue, and inflammatory mediators are shown in pink. The merged colors indicate the contribution of each pathway to BBB breakdown and inflammation. Pathological events occurring in the CNS by local injuries or in the periphery, induced by infections or autoimmune disorders, lead to the activation of brain cells or leukocytes, respectively.

The activated cells secrete inflammatory mediators in the brain or blood that initiate a cascade of inflammatory events with a broad variety of physiopathological outcomes. The effects of brain inflammation play a key role in seizure generation and cell death that in turn, evokes further inflammation, resulting in a vicious circle of events that participate in the development of epilepsy. Abbreviations: AP1, activator protein 1; BBB, blood–brain barrier; COX, cyclooxygenase; GABA, γ -aminobutyric acid; HMGB1, high-mobility group box 1; MAPK, mitogen-activated protein kinase; NF κ B, nuclear factor kappa B; PI3K, phosphoinositide 3-kinase; PLA2, phospholipases A2; TGF- β , transforming growth factor β ; TNF, tumor necrosis factor (Vezzani et al., 2011).

1.6 Microglial nodules – common feature among inflammatory CNS diseases

Microglial nodules are common findings in various neurological diseases, for example viral encephalitis or chronic inflammatory diseases such as multiple sclerosis (MS) and Rasmussen encephalitis. The activated microglia often cluster around infected neurons, invade and digest them, a process called neuronophagia (Haberland, 2006). In MS, microglial nodules in the normal-appearing white matter might represent the earliest stage of lesion development and were therefore named pre-active lesions (De Groot et al., 2001). Nevertheless, these nodules are recognized in the absence of leukocyte infiltration, astrogliosis or demyelination, but may develop into active demyelinating lesions (van Noort et al., 2010). Furthermore, these nodules seem to be associated with altered or damaged axons in early MS (Singh et al., 2013).

So far, little is known about the composition and role of microglial nodules in RE and there is only limited literature available. My preceding colleague performed the quantification of IL-1 β and was able to show that IL-1 β mRNA and protein levels were increased in RE compared to the control group. Moreover, immunohistochemical stainings for IL-1 β exposed that IL-1 β was present in microglial nodules in samples derived from RE patients.

Until now, it is known that microglia activation and formation of nodules can occur in the cortex as well as the white matter of RE patients (Ramaswamy et al., 2013).

Some years ago, the transmembrane protein 119 (Tmem119) was identified as a new microglia specific marker in humans and mice. The protein is only expressed on Iba1⁺CD68⁺ microglia with a ramified and amoeboid morphology, which indicates phagocytic activity, and not found in blood-derived macrophages (Singh et al., 2013). With the help of Tmem119 immunohistochemistry, studies on microglia pathology and microglial nodules in RE were facilitated.

1.7 The Inflammasome

Several pathways can trigger the stimulation of the innate immunity in the CNS after the detection of invading pathogens and tissue damage by pattern recognition receptor (PRRs). In the last decade, researchers focused on the two-signal model mediated by toll-like receptors (TLRs) and nucleotide binding and oligomerization domain (NOD)-like receptors (NLRs). TLRs and NLRs detect pathogen-associated molecular patterns (PAMPs) or DAMPs released as a reaction to cell stress or injury. NLRs are intracellular sensors that contribute to the formation of the inflammasome, which is responsible for the processing of the pro-inflammatory cytokines pro-IL-1 β and pro-IL-18 (Hanamsagar et al., 2012). The inflammasome is a multiprotein complex involved in the activation of caspase 1 after infections, injuries or in autoimmune diseases (de Rivero Vaccari et al., 2014). The activated caspase 1 then converts the pro-IL-1 β and pro-IL-18 into their mature and active forms, which leads to the induction and amplification of downstream signaling pathways and proinflammatory reactions, resulting in cellular damages like autophagy and pyroptosis (Schroder and Tschopp, 2010; Zhou et al., 2016). Pyroptosis is a caspase 1 mediated cell death that appears to be associated with inflammasome activation (E. Vince and Silke, 2016).

The inflammasomes are composed of NLRs that usually have 1) a central nucleotide-binding and oligomerisation (NACHT) domain; 2) a variable number of C-terminal leucine rich repeat (LRR) motifs for the sensing of pathogenic molecules; and 3) an N-terminal caspase activation and recruitment domain (CARD) or a pyrin domain (PYD) for binding adaptor and effector proteins (Edye et al., 2014; Lamkanfi and Dixit, 2009).

So far, 2 distinct types of inflammasomes have been characterized. The first type is the NLR-family, which includes NLRP1, NLRP3 and NLRC4. The second inflammasome employs the AIM2 (absent in melanoma 2) protein which is a member of the non-NLR family and consists of a pyrin and DNA-binding HIN domain (van de Veerdonk et al., 2011).

The most thoroughly studied inflammasome is the NLRP3 (also referred to as NALP3 or cryopirin) inflammasome (Figure 3), which is considered to have a pivotal role in CNS pathologies. It consists of the NLRP3 scaffold, the adaptor apoptosis-associated speck-like protein (ASC) and pro-caspase 1 (Schroder and Tschopp,

2010; Zhou et al., 2016). NLRP3 is the sensor element that is located in the cytoplasm. The oligomerization of NLRP3 leads to the autoproteolytic activation of pro-caspase 1 converting the zymogen into its mature form (Agostini et al., 2004). Caspase 1 mediates the cleavage of pro-IL-18 and pro-IL1 β into their highly pro-inflammatory mature forms, which then mediate immune responses (Keller et al., 2008)

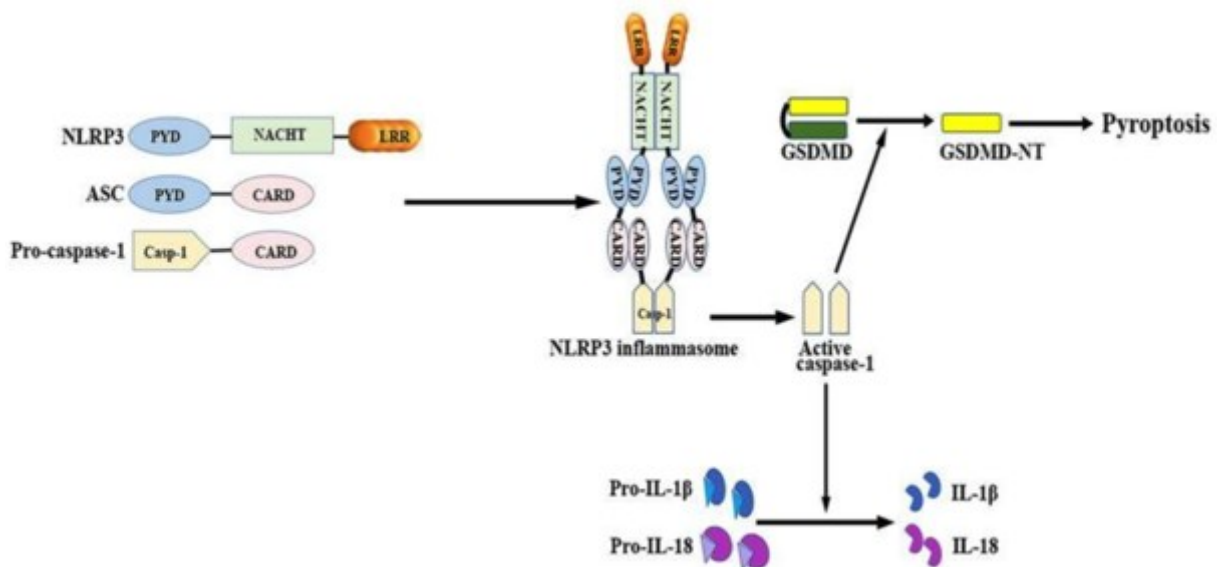


Figure 3. Structure and function of the NLRP3 inflammasome (Song et al., 2017). The components of the inflammasome are the cytosolic NLRP3 molecule, the adaptor protein ASC and the effector molecule pro-caspase 1. The mature caspase 1 converts the inactive forms of IL-1 β and IL-18 into their active forms. ASC, apoptosis-related speck-like protein containing a caspase recruitment domain; CARD, caspase activation and recruitment domain; GSDMD, gasdermin D; GSDMD-NT, gasdermin-N domain of GSDMD; IL, interleukin; LRR, leucine-rich repeat; NACHT (NOD), nucleotide binding and oligomerization domain; NLRP3, nucleotide-binding oligomerization domain-, leucine-rich repeat- and pyrin domain-containing 3; PYD, pyrin-only domain (Agostini et al., 2004; Song et al., 2017) .

The NLRP3 inflammasome appears to be activated by two signals: the priming step affects the transcriptional process of NLRP3 and pro-IL-1 β by induction of the NF κ B pathway. Ligands for TLRs trigger a signaling cascade that results in the activation of the transcription factor NF κ B, which enhances the transcription of NLRP3 and pro-IL-1 β . The second step required is the activation of the inflammasome by an endogenous or exogenous ligand, stimulating PAMPS or DAMPS, that leads to the assembly and initiation of the inflammasome. 3 main mechanisms were suggested for NLRP3 activation, which are shown in Figure 4, that ultimately result in the

cleavage of pro-caspase 1 into the active caspase 1 (Sutterwala et al., 2014; Zhou et al., 2016).

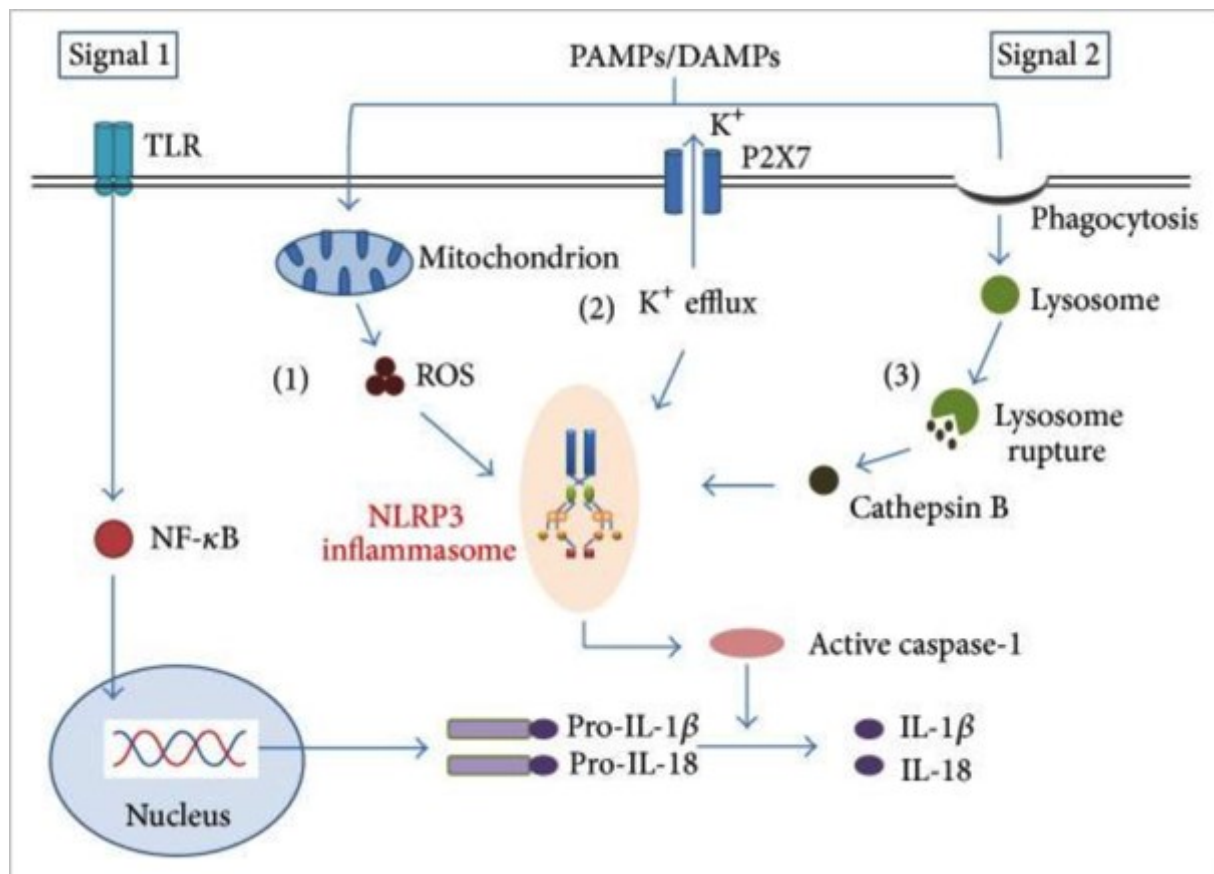


Figure 4. NLRP3 inflammasome activation models. Signal 1 stimulates the transcription of NLRP3 and pro-IL-1 β via the TLR/NF κ B pathway. Signal 2 is mediated by PAMPs or DAMPs and culminates in the assembly of the inflammasome. So far, there are 3 different main mechanisms of inflammasome activation. (1) Stimuli can provoke the production of mitochondrial ROS and induce the NLRP3 inflammasome activity. (2) The reduction of intracellular K⁺ concentrations, induced by extracellular ATP or bacterial toxins, leads to the inflammasome activation. (3) The rupture of lysosomes, by phagocytosis of particular crystals, and the subsequent release of lysosomal contents can induce the inflammasome activation (Zhou et al., 2016).

In addition to the described main mechanisms for activation of the NLRP3 inflammasome, there is growing evidence that one signal alone is not enough to induce the inflammasome (Gross et al., 2011). Numerous other pathways were investigated by researchers and may elucidate the mechanisms by which various stimuli activate the inflammasome (Zhou et al., 2016).

The function of the inflammasomes in the healthy and diseased CNS has received major attention in the past years. For example, the NLRP1 inflammasome is found in the motor neurons of the spinal cord and in cortical neurons. An increasing amount of studies demonstrated that the NLRP3 inflammasome is expressed in diverse cells such as microglia, astrocytes, neurons, endothelial cells (Lammerding et al., 2016; Lu et al., 2014; Nagyószzi et al., 2015) and different types of diseases like TBI, stroke, brain tumors and neurodegenerative disorders (Zhou et al., 2016). Since studies revealed that neuroinflammation is associated with epileptogenesis, researchers also verified that the NLRP3 inflammasome plays a crucial role in epilepsy. Thus, the inhibition of the inflammasome might be an important therapeutic approach for preventing neuronal damage and neuroinflammation after seizures (Meng et al., 2014).

Regarding RE, components of the inflammasome are mostly produced in microglia and macrophages, and the highest inflammasome activation and release of interleukins was observed in microglia, but not astrocytes. Furthermore, expression of NLRP3 and other inflammasomes such as NLRP1 are increased in brain tissue samples from RE patients compared to the control group (Ramaswamy et al., 2013).

1.8 Interleukin-18 and its role in neuroinflammation

IL-18, first described as “IFN γ -inducing factor”, is a member of the IL-1 superfamily and plays an important role in the innate and adaptive immunity. It is one of the cytokines that is processed into its mature form by the NLRP3 inflammasome. For a long time, the contribution of IL-18 in neuroinflammation has not been completely understood (Alboni et al., 2010; Dinarello, 1999).

IL-18 mRNA was detected in various different brain regions like the hypothalamus, hippocampus, striatum, cerebellum and cerebral cortex (Culhane et al., 1998). The main source of IL-18 are activated microglia and researchers found elevated concentrations of IL-18 and IL-1 β in the cerebrospinal fluid (CSF), brain tissue and blood plasma of patients with different CNS disorders, such as MS, brain injury and CNS infection (de Jong et al., 2002; Huang et al., 2004). Once secreted, both cytokines bind to their receptors on microglia, neurons, astrocytes and endothelial cells, stimulating various signaling pathways, which leads to further expression of genes associated with inflammation (Song et al., 2017).

The role of IL-18 and caspase 1 as potential participants in acute and chronic neurodegeneration was extensively studied. Early data retrieved from an experimental autoimmune encephalomyelitis (EAE) model in rats revealed an increase in IL-18 and caspase 1 expression in the CNS during the acute stage of disease (Jander and Stoll, 1998). Another study demonstrated that IL-18 enhances the severity of EAE in the mouse model (Shi et al., 2000).

Besides, IL-18 also activates signaling events in microglial cells, which cause elevated caspase 1 expression and pro-inflammatory cytokine production (e.g. IL-1 β and IFN γ) (Felderhoff-Mueser et al., 2005). A unique feature of IL-18 is the exacerbation of Fas-mediated neuronal cell death, by enhancing the expression of the Fas ligand in glial cells (Song et al., 2017). Furthermore, IL-18 deficient mice exhibited impaired microglia activation in combination with altered phagocytic functions leading to diminished clearance of neurovirulent influenza A virus (Mori et al., 2001).

Beyond the CNS, IL-18 stimulates the production of chemokines, adhesion molecules and further pro-inflammatory cytokines in natural killer cells, Th1 and B cells (Bossù et al., 2010; Nakahira et al., 2002). The most prominent biological property of IL-18 is the ability of inducing IFN γ , in synergism with IL-12 or IL-15, in T cells and natural killer cells (Okamura et al., 1995).

The involvement of IL-18 in different immune responses leads to the conclusion that the cytokine is not only important for the host defense against intracellular infection, but also for the regulation of the production of pro-inflammatory cytokines (Dinarello, 1999).

1.9 Objectives of the thesis

Since the primary cause of RE is still not known, the research on the underlying process that triggers inflammation is of great interest. RE is a rare disorder with heterogeneous pathological modifications, but histological findings suggest that microglial changes, death of neurons and glia are the earliest components (Pardo et al., 2004). Preceding work on this project has already been accomplished by my colleagues, who analyzed the cytokine IL-1 β and its receptor in RE.

It was now my task to study the pro-inflammatory cytokine IL-18 and caspase 1, which are components of the inflammasome, in RE and MTLE. Furthermore, we

were interested in the characterization of microglial nodules in the cortex of RE patients. Thus, the aims of this thesis were:

- The quantification of RNA transcripts of IL-18 and caspase 1 in RE, MTLE and control group.

To achieve this, quantitative real-time PCR of RE, MTLE and control samples was performed after RNA isolation from FFPE tissue.

- The quantification and detection of IL-18 at protein level in RE and MTLE. The cytokine IL-18 was quantitatively evaluated by performing immunohistochemistry in RE and MTLE tissue and compared to the controls.

- Analyzing if IL-18 and caspase 1 are expressed differently in RE and MTLE. The obtained data were statistically evaluated to find out whether the RNA and protein levels of IL-18 and caspase 1 are changed in RE stages and MTLE compared to the control group.

- The analysis of microglial nodules in RE and their properties.

Different immunohistochemical stainings for light and confocal microscopy were performed to detect the nodules and analyze them. Additionally, the amount of microglia and T cells per nodule were counted to determine whether microglial activation precedes T cell infiltration.

2 Materials and Methods

2.1 Human Study Samples

The study was performed on a collection of formalin-fixed, paraffin-embedded (FFPE) human brain tissue from patients suffering from one of the following diseases: Rasmussen encephalitis (RE, n = 23), virus-induced encephalitis (n = 21) and mesial temporal lobe epilepsy (MTLE, n = 7). Some samples derived from patients that developed MTLE after suffering from viral encephalitis, which are termed MTLE + Enc (n = 4) in this thesis. In addition, 10 control samples were used; 2 were healthy autopsy controls and 8 were epileptic controls derived from resection of epileptic brain tissue. Detailed clinical data from included patients are listed in Table 1 in the appendix.

The RE samples were grouped into 4 different stages of disease: Stage 0, 1, 2 and 3. Staging was performed based on the evaluation of histopathological hallmarks of RE, namely neuroinflammation and neurodegeneration. To this end, immunohistochemical stainings were performed for markers for T cells (CD3), microglia (CD68) and neurons (NeuN).

2.2 Deparaffinization

2.2.1 Materials

3-5 µm thick FFPE sections mounted on microscope glass slides

Xylene (J. T. Baker)

Ethanol (EtOH) 96%, 70%, 50% (Brenntag)

Distilled water (a.d., aqua destillata)

2.2.2 Method

The slides were deparaffinized, blocked and rehydrated. In the beginning, the FFPE samples were dewaxed by incubation in xylene twice for 15 minutes and washed in 96% ethanol. Then the endogenous peroxidase activity was blocked by incubation in H₂O₂/Methanol for 30 minutes at room temperature. This step was only done for immunohistochemistry, but skipped for the hematoxylin-eosin staining. Afterwards, they were rehydrated in a descending alcohol series through 96% ethanol, 70% ethanol, 50% ethanol and distilled water.

2.3 Hematoxylin-Eosin (HE) staining

2.3.1 Materials

HCl-Ethanol

0.5 ml 37% HCl (Sigma-Aldrich)
+ 100 ml 70% ethanol

Scott's solution

2 g KHCO₃ (Merck)
+ 20 g MgSO₄ x 7H₂O (Merck)
+ 1 L a.d.

Mayer's Hemalaun (Merck)

Coverslips (Kindler)

Eukitt (Sigma)

Eosin stock solution

10 g Eosin
+ 100 ml a.d.

Let stand for some days

Eosin working solution

250 ml of 1:100 dilution of eosin stock
+ 12 drops glacial acidic acid

2.3.2 Method

After dewaxing, the slides were subsequently incubated in Mayer's hemalaun for 5 minutes for the nuclear staining. After washing with tap water, the slides were differentiated in HCl-ethanol and again washed with water. Next, the sections were incubated 5 minutes in Scott's solution and rinsed with tap water. For the cytoplasmic staining, incubation of 4 minutes in Eosin solution was performed and afterwards washed with water. In the final step, the slides were dehydrated through the ascending ethanol series (50%, 70%, 3x 95%) and n-butyl acetate. For mounting, coverslips and Eukitt was used.

2.4 Immunohistochemistry

2.4.1 Single staining for light microscopy

2.4.1.1 Materials

3-5 µm thick FFPE sections mounted on microscope glass slides

Xylene (J. T. Baker)

Ethanol (EtOH) 96%, 70%, 50% (Brenntag)

Primary antibodies (Table 2)

Secondary antibodies (Table 3)

Avidin–horse radish peroxidase (Jackson Immunoresearch)

Mayer's Hemalaun (Merck)

Coverslips (Carl Roth, Kindler)

Eukitt (Sigma)

Hydrogen peroxidase (H₂O₂)/Methanol

150 ml Methanol (Sigma-Aldrich)
+ 1 ml of 30% H₂O₂ (VWR)

TBS stock solution, pH 7.5

180 g 150 mM NaCl (VWR)
+ 60.57 g 25 mM Tris buffer (VWR)
+ 400 ml 1 N HCL (Sigma-Aldrich)

Fill up to 1 L with distilled water

Adjust pH to 7.5 with 1 N HCl

TBS working solution

Dilute stock solution 1:20 with a.d.

PBS stock solution, pH 7.4

13.8 g 0.04 M NaH₂PO₄ (VWR)
+ 71.2 g 0.16 M Na₂HPO₄ (VWR)
+ 90 g NaCl

Fill up with a.d. to 2.5 L

The pH was adjusted to 7.4

PBS working solution

Dilute stock solution 1:4 with a.d.

10% fetal calf serum (FCS)/Dako buffer

10x Dako buffer solution (Dako corporation) was diluted 1:10 with distilled water. For antibody and avidin peroxidase incubation, a mixture of 10% FCS (Gibco) in Dako buffer was used.

EDTA stock solution

1.21 g 10 mM Tris-buffer (VWR)
+ 0.37 g of 1 mM EDTA (VWR)
+ 50 ml a.d.

The pH was either adjusted to 8.5 or 9.0, depending on the fixation of used material.

EDTA working solution

2.5 ml of stock solution
+ 47.5 ml a.d.

Catalyzed signal amplification (CSA) stock

6 ml borate buffer (0.1545 g boric acid (Merck) in 50 ml a.d.; adjust pH with NaOH to 8.0)
+ 15 mg sulfo-NHS-LC-Biotin (Pierce)
+ 4.5 mg tyramine (Sigma)

Stir overnight at room temperature

Filter and store 20 µl aliquots at -20°C

CSA Working solution

Dilute aliquot in 20 ml PBS
+ 20 µl 30% H₂O₂

DAB (3,3'-Diaminobenzidine)

Stock solution

1 g 3,3' DAB (Sigma-Aldrich)
+ 40 ml PBS

1 ml aliquots stored at -20°C

Working solution

1 ml aliquot
+ 50 ml PBS buffer
Filter
+ 16.5 µl H₂O₂

HCl-Ethanol

0.5 ml 37% HCl (Sigma-Aldrich)
+ 100 ml 70% ethanol

Scott's solution

2 g KHCO₃ (Merck)
+ 20 g MgSO₄ x 7H₂O (Merck)
+ 1 L a.d.

Primary Antibody (Ab)	Ab type	Target	Pretreatment	Dilution	Source
Interleukin-18 (IL-18)	Rabbit, polyclonal	Human IL-18	Steamer 60' EDTA 8.5	1:2000	Abcam (#191152)
P-Stat1	Rabbit, monoclonal	Phosphorylated Stat1	Steamer 60' EDTA 9.0	1:2000 + CSA	Cell signaling (#9167)
CD3	Rabbit, polyclonal	T cells	Steamer 60' EDTA 9.0	1:500	Dako (A0452)
CD8	Mouse, monoclonal	Cytotoxic T cells	Steamer 60' EDTA 9.0	1:250 + CSA	Dako (M7103)
Iba1	Rabbit, polyclonal	Microglia and macrophages	Steamer 60' EDTA 9.0	1:3000	Wako (#019-19741)
Caspase 1	Rabbit, polyclonal	Human Caspase 1	Steamer 60' EDTA 8.5	1:5000	Proteintech (#22915-1-A)

Table 2. Overview of primary antibodies used for IHC.

Secondary Antibodies	Target	Dilution	Source
Bi-donkey- α -rabbit	IgG (H+L)	1:2000	Jackson ImmunoResearch (#711-065-152)
Bi-donkey- α -mouse	IgG (H+L)	1:1500	Jackson ImmunoResearch (#715-065-150)

Table 3. Secondary antibodies for IHC.

2.4.1.2 Method

The immunohistochemical stainings were done as single or double labeling using primary antibodies and biotinylated secondary antibodies. Single stainings were performed for IL-18 on controls, RE and MTLE cases. RE cases were stained for Caspase 1. Double stainings were done on samples from patients suffering from RE and virus-induced encephalitis. All incubations were performed in a humid chamber to keep the slides from drying out.

First, the slides were deparaffinized as described above. For pretreatment, heat induced antigen retrieval was done by steaming in a common household steamer (MultiGourmet FS20; Braun, Kronberg/Taunus, Germany) using EDTA (pH = 8.5 or 9) or citrate buffer (pH = 6). The appropriate solution and duration were chosen depending on the used antibody (see Table 2). The slides were washed 3-5 times with TBS buffer, after cooling down to room temperature. Next, unspecific background reactions were reduced by blocking with 10% FCS/Dako buffer in a

humid chamber at room temperature for 15 minutes. Afterwards, the slides were incubated with the primary antibody in appropriate dilution (see Table 2) in 10% FCS/Dako buffer at 4°C overnight. Next day, they were washed 3-5 times in TBS buffer and subsequently incubated with the biotinylated secondary antibody (see Table 3) diluted in 10% FCS/Dako buffer, in a humid chamber for 1 hour at room temperature. Again, the slides were rinsed in TBS 3-5 times, followed by 1 hour incubation with streptavidin-peroxidase diluted 1:500 in 10% FCS/Dako buffer, at room temperature. In case of Stat1, signal enhancement with biotinylated tyramine was needed. Therefore these samples were incubated for 20 minutes in CSA working solution after the streptavidin-peroxidase, followed by washing with PBS. Once more, streptavidin-peroxidase was applied for 30 minutes and afterwards washed with TBS. Afterwards, the samples were developed with DAB under microscopic control. The enzymatic reaction was stopped with deionized water. Counterstaining of the slides was performed by 20 seconds incubation in Mayer's hemalaun, rinsing in tap water and differentiation in HCl-ethanol. The slides were again washed with tap water, incubated in Scott's solution for 3 minutes and rinsed in tap water. As a result, the nuclei of all cells are stained blue. Finally, the slides were dehydrated in the ascending ethanol series (1x 50%, 1x 70% and 3x 90%) and n-butyl acetate and coverslipped with Eukitt. After the slides were dried, they were examined under the microscope.

2.4.2 Double stainings for light microscopy

2.4.2.1 Materials

In general, the materials for double stainings are the same as for single stainings, except some more solutions were needed in addition:

Avidin–alkaline phosphatase (AP) (Jackson Immunoresearch)

Aquatex (Merck)

Citrate buffer, pH 6.0

2.10 g 1 M citric acid (Sigma-Aldrich)
+ 1 L a.d.

Fast Blue solution (50 ml)

6.25 mg naphthol-AS-MX-Phosphate (Sigma)
+ 308 µl dimethylformamide
+ 50 ml warm Tris/HCL buffer (0.1 M, pH 8.5)
12.5 mg Fast Blue BB salt (Sigma)

+ 308 μ l 2 N HCl
+ 308 μ l 4% NaNO₂
Add to Tris/HCl mix
+ 77 μ l 1 M levamisole
Incubate shortly, filtrate

Fast Red solution (50 ml)

Tris stock solution (0.1 M, pH 8.2)

12.1 g Tris (VWR)
+ 920 ml a.d.
Add 1 N HCl until pH is 8.2

0.2 g Naphtol-AS MX phosphate
+ 20 ml dimethylformamide
+ 980 ml Tris stock (0.1 M, pH 8.2)
+ 1 ml 1 M levamisole

Mix and aliquot in 50 ml falcon tubes

Store at -20°C

Working solution

Thaw 1 aliquot (50 ml)
+ 0.05 g Fast Red TR Salt (Sigma)
Filtrate

DAB Nickel

DAB working solution
+ 1 ml 1% ammoniumnickelsulfate (Sigma)
+ 0.6 ml 1% cobalt(II)chloride (VWR)

Geltol

60 g glycerol
+ 24 g mowiol

Mix for at least 30 minutes

+ 60 ml a.d. and incubation at room temperature for 2 hours
+ 120 ml Tris (0.2 M, pH 8.5)

Heat up to 50°C, stir for 10 minutes

Fill in falcon tubes

Centrifuge 15 minutes at 5000 \times g

Storage at -20°C

2.4.2.2 Method

The deparaffinization, pretreatment and application of the primary and secondary antibody were the same as described earlier. Since the antibodies for the double labelings originate from the same species (i.e. CD3 and Iba1), stainings have to be

performed on three consecutive days with each antibody presented separately to the tissue. The first antibody is presented overnight and developed with fast blue using alkaline phosphatase activity for detection. Therefore, slides were incubated with avidin-alkaline phosphatase (AP) (1:500) instead of streptavidin-peroxidase for 1 hour at room temperature. For visualization, the Fast Blue solution was prepared and slides were incubated at 37°C. The reaction was then stopped with a.d. Subsequently, the slides were steamed again for 30 minutes in citrate or EDTA buffer to remove the unbound components from the first labeling and avoid cross-reactions in the second staining. After steaming and washing with TBS, the slides were incubated with the second primary antibody overnight at 4°C. On the final day of the staining protocol, the secondary antibody and streptavidin-peroxidase incubations were performed as mentioned above. DAB was used for visualizing the second labeling and the reaction was again stopped with a.d. In this case only a weak counterstain was performed, in order to be able to distinguish the hematoxylin and fast blue signals. The slides were then mounted using geltol and coverslips.

Due to difficulties in distinguishing the Fast Blue staining and counterstaining of the nuclei while trying to count microglia, a double staining using Fast Red for the first detection and DAB nickel for the second detection was performed. The same protocol as described was applied, and the counterstaining was done as usual. As a result, the proteins of interest appear reddish (Fast Red) and black (DAB nickel).

2.5 Confocal Laser Fluorescence Microscopy

2.5.1 Materials

3-5 µm thick FFPE sections mounted on microscope glass slides

Xylene (J. T. Baker)

Ethanol (EtOH) 96%, 70%, 50% (Brenntag)

TBS working solution

EDTA working solution

10% FCS/Dako buffer

Dako Real™ Antibody Diluent

Primary antibodies (Table 4)

Secondary antibodies (Table 5)

Streptavidin conjugated Cy2 (Jackson Immunoresearch)

Coverslips (Carl Roth)

Confocal LEICA SP5 DMI 6000 CS laser scan microscope (Mannheim, Germany)

CSA working solution

Dilute aliquot in 20 ml PBS
+ 20 µl 30% H₂O₂

Gallate/geltol

10 ml Geltol
+ 0.2 g Gallate (0.1 M)
Stir overnight and store at 4°C

Primary Antibody (Ab)	Ab type	Target	Pretreatment	Dilution	Source
IL-18	Rabbit, polyclonal	Human IL-18	Steamer 60' EDTA 8.5	1:5000	Abcam (#191152)
CD68	Mouse, monoclonal	Tissue macrophages and microglia	Steamer 60' EDTA 8.5	1:50	Dako (M0814)
Iba1	Rabbit, polyclonal	Microglia and macrophages	Steamer 60' EDTA 9.0	1:10000 + CSA	Wako (#019-19741)
Tmem119	Rabbit, polyclonal	Microglia	Steamer 60', EDTA 9.0	1:150	Sigma (#HPA051870)

Table 4. Primary antibodies used for fluorescence IHC.

Secondary Antibodies	Target	Dilution	Source
Bi-donkey-α-rabbit	IgG (H+L)	1:2000	Jackson ImmunoResearch (#711-065-152)
Cy3 donkey-α-mouse	IgG (H+L)	1:100	Jackson ImmunoResearch (#715-165-151)

Table 5. Secondary antibodies.

2.5.2 Method

As described for the light microscope stainings, the slides were deparaffinized in xylene, blocked with hydrogen peroxidase and rehydrated. For antigen retrieval, the optimal steaming buffer and time was chosen depending on the antibody. After washing with TBS, unspecific background signals were blocked with Dako Real™ Antibody Diluent for 20 minutes. Subsequently the slides were incubated with the primary antibody overnight at 4°C. The antibodies were diluted according to Table 4 in the Dako Real™ Antibody Diluent. Next day, the slides were rinsed in TBS and incubated with the secondary antibody (Table 5) that was diluted in 10% FCS/Dako buffer for 1 hour, followed by incubation with streptavidin-Cy2 diluted 1:100 in 10% FCS/Dako buffer for 1 hour in the dark. In case the antibody needs signal enhancement, the slides were incubated with streptavidin-peroxidase, instead of streptavidin-Cy2. Next, CSA was applied on the sections for 20 minutes, followed by a washing step with TBS. The sections were then steamed for 30 minutes in EDTA buffer, before another incubation with streptavidin-Cy2 for 30 minutes, and lastly rinsed with TBS. After this step, the second primary antibody from the same species was diluted in 10% FCS/Dako buffer and applied on the slides overnight at 4°C. Then, a secondary antibody directly conjugated with a fluorophore (e.g. Cy3), diluted in 10% FCS/Dako buffer, was applied on the slides for 1 hour protected from light. Lastly, slides were washed with a.d. and mounted with gallate/geltol. The finished slides needed to be stored at 4°C until they were studied with the confocal microscope. When the mounting medium was dried, the stainings were examined with the LEICA TCS SP5 laser scan microscope (Leica Mannheim, Germany) with lasers for 488 and 543 nm excitation. The scanning was performed sequentially for Cy2 (488 nm) and Cy3 (543 nm).

2.6 RNA Isolation

2.6.1 Materials

7-8 µm thick FFPE sections (RNase-free)

Xylene (J. T. Baker)

Ethanol (EtOH) 96%, 70% (Brenntag)

1.5 ml Eppendorf tubes (RNase-free)

0.6 ml Eppendorf tubes (RNase-free)

High Pure FFPE RNA Micro Kit (Roche)

Ethanol absolute (Merck)

Sterile disposable scalpels, Cutfix® (B. Braun)

UltraPure™ DNase/RNase-free distilled water (ThermoFisher Scientific)

RNase Zap™ (ThermoFisher Scientific)

10% Sodium dodecyl sulfate (SDS) (Alfa Aesar)

Lysis buffer: 60 µl tissue lysis buffer mixed with 10 µl 10% SDS

Centrifuge 5415D (Eppendorf)

Centrifuge Sigma 1-14 (Linder Labortechnik)

Fume hood (SM Labortechnik)

2.6.2 Method

For isolation of RNA, three sections were cut, two of which were used for isolation and one, stained with H&E, was used as template. Isolation was performed according to the manufacturers instructions, with slight modifications. The isolation was performed in a fume hood (SM Labortechnik) to guarantee RNase-free conditions and avoidance of contamination. After examining the HE stained sections, regions of interest were marked. Selected regions with RNA from the brain tissue were scratched from the slides with a scalpel and collected in Eppendorf tubes. This material was deparaffinized by incubation with xylene for 2 minutes followed by 3 times 4 seconds vortexing and another 5 minutes incubation with xylene (see Table 6). The samples were then centrifuged for 2 minutes at maximum speed (13200 rpm) to collect the pellet at the bottom of the tubes. The xylene was removed carefully, avoiding aspirating the pellet. This process of xylene incubation was repeated once. Afterwards, the samples were incubated first with ethanol absolute followed by 70% EtOH for rehydration. To clear residual EtOH, samples were centrifuged shortly and air-dried for 20 minutes in the incubator at 55°C with an open lid. When the remaining EtOH was evaporated, 60 µl of lysis buffer, 10 µl 10% SDS and 30 µl proteinase K were added immediately to each tube and mixed properly as described in Table 6

(Steps 11-13). After this, the samples were incubated at 55°C for 10 hours, followed by 20 minutes at 70°C. Finally, the samples were stored at -80°C until continuation of the experiment.

Next, the samples were thawed and placed in an ice box. EtOH absolute and binding buffer was added to each sample, vortexed and centrifuged for 1 minute at 8000 ×g. Using the High Pure FFPE RNA Micro kit by Roche, filter and collection tubes were prepared. The lysates were applied in the upper compartment of the spin column and tubes were centrifuged allowing the solution to flow-through (Table 6; steps 15-20) for 30 seconds at 8000 ×g. The flow-through was discarded, and samples were again centrifuged for 1 minute at maximum speed. The rest of the flow-through was discarded and the DNase solution was prepared. For each sample, 27 µl DNase I and 3 µl DNase incubation buffer were mixed and added. After an incubation time of 15 minutes at room temperature, several washing steps with washing buffer I and II and centrifugation were performed (Steps 22-30). Finally, filter tubes were placed in 1.5 ml Eppendorf tubes and elution buffer was added. After the elution procedure, the eluate was transferred in fresh tubes and 2 µl RNA aliquots were taken for analysis with an Agilent 2100 Bioanalyzer.

RNA isolation protocol

1. Add 800 μ l xylene, vortex 4 sec (3x)
2. Incubate 2 min, vortex 4 sec (3x)
3. Incubate 5 min, centrifuge 2 min (max speed)
4. Remove xylene without damaging tissue pellet
5. Repeat xylene steps
6. Add 800 μ l EtOH absolute, vortex 4 sec (3x)
7. Centrifuge 2 min (max speed), remove EtOH absolute
8. Add 800 μ l 70% EtOH, vortex 4 sec (3x)
9. Centrifuge 2 min (max speed), remove EtOH
10. Centrifuge again 30 sec (max speed), remove remaining EtOH
11. Airdry 20 min at 55°C in incubator until EtOH completely vaporized
12. Add 70 μ l of lysis buffer + 30 μ l Proteinase K, mix properly
13. Incubate for 10 hours at 55°C, then 20 min at 70°C
14. Place samples in ice box
15. Add 200 μ l binding buffer + 200 μ l 100% EtOH
16. Vortex 4 sec (3x), spin down 1 min (8000 \times g)
17. Prepare filter and collection tubes from Roche
18. Pipet lysate in upper parts
19. Centrifuge 30 sec (8000 \times g), discard flowthrough
20. Centrifuge 1 min (max speed), discard flowthrough
21. Add 30 μ l DNase Solution (27 μ l DNase I + 3 μ l DNase incubation buffer)
22. Incubate for 15 min at room temperature
23. Add 300 μ l washing buffer I
24. Centrifuge 15 sec (8000 \times g), discard flowthrough
25. Add 300 μ l washing buffer II
26. Centrifuge 15 sec (8000 \times g), discard flowthrough
27. Add 200 μ l washing buffer II
28. Centrifuge 15 sec (8000 \times g), discard flowthrough
29. Place filter tubes in new collection tubes
30. Centrifuge 2 min (max speed)
31. Place filter tubes in fresh 1.5 ml Eppendorf tubes
32. Add 20 μ l elution buffer, incubate 1 min at room temperature
33. Centrifuge 1 min (8000 \times g), reload eluate, repeat incubation + centrifugation
34. Centrifuge 2 min (max speed), transfer eluate in new tubes, take 2 μ l aliquot
35. Store at -80°C

Table 6. Detailed protocol for RNA isolation with the High Pure FFPE RNA Micro Kit from Roche.

2.6.3 RNA Quality Measurement

The Bioanalyzer creates an electropherogram and determines the RNA integrity, area under the curve and RNA concentration. RNA concentration is measured in the range of 50 pg/μl to 5 ng/μl. RNA integrity is given as RNA integrity numbers (RIN). For FFPE samples, the quality is evaluated by the RNA concentration and DV200 value. The DV200 value is a parameter used for the percentage of RNA fragments longer than 200 nucleotides in a sample. Samples with values above 70% can be considered as high quality RNA. Since sufficiently long RNA fragments are necessary for successful qPCR, samples with concentrations higher than 500 pg/μl were chosen for further applications. In case that a sample showed insufficient RNA concentration or quality, the RNA isolation process had to be repeated.

2.7 Reverse Transcription PCR

2.7.1 Materials

RNA samples

iScript™ cDNA Synthesis Kit (Bio-Rad)

1.5 ml Eppendorf tubes (RNase-free)

0.2 ml PCR soft tubes DNase/RNase-free (Biozym)

MyFuge™ Mini centrifuge (Benchmark Scientific)

Fume hood (Holten LaminAir)

MyCycler™ Thermal Cycler (Bio-Rad)

2.7.2 Method

Reverse transcription is a necessary process to transcribe the isolated RNA into complementary DNA (cDNA). The reagents were thawed, vortexed shortly and put on ice. Then, a master mix of 5x iScript reaction mix and reverse transcriptase was made as described in Table 7. The required volume of RNA, for each sample, was calculated to reach a final concentration of 4 ng per 20 μl. For a total volume of 20 μl, nuclease-free H₂O was added to the samples. As a negative control, 5 μl of the master mix were added to 15 μl nuclease-free H₂O. All samples were incubated in the thermal cycler (Bio-Rad) for 5 minutes at 25°C, then at 42°C for 30 minutes and

finally for 5 minutes at 85°C. The cDNA samples were stored at 4°C for qPCR in the near future, otherwise kept at -20°C, when not used for further experiments.

Component	Volume per reaction
5x iScript reaction mix	4 µl
Reverse transcriptase	1 µl
RNA sample	x µl
Nuclease-free H₂O	x µl
Total reaction volume	20 µl

Table 7. Reaction mix for reverse transcription.

2.8 Quantitative Real-Time PCR

2.8.1 Materials

cDNA samples

Sso Advanced™ Universal SYBR® Green Supermix (Bio-Rad)

Forward and reverse Primer (Eurofins Genomics)

0.2 ml PCR soft tubes DNase/RNase-free (Biozym)

Multiplate PCR plates 96-well (Bio-Rad)

Microseal 'B' seals (Bio-Rad)

UltraPure™ DNase/RNase-free distilled water (ThermoFisher Scientific)

0.6 ml Eppendorf tubes (RNase-free)

StepOne Plus Real-Time PCR System (Applied Biosystems)

StepOne software v2.2.2. (Applied Biosystems)

Fume hood (Holten LaminAir)

2.8.2 Method

Quantitative real-time PCR was carried out for quantification of interleukin-18 and caspase 1 mRNA in control and disease samples. In order to normalize the results, the housekeeping gene GAPDH was used as a reference. The chosen primers for IL-18 and caspase 1 bind at the 3' end, therefore 3' primers were also used for the housekeeping gene GAPDH (see Table 8).

Gene		Forward Primer 5'-> 3'	Reverse Primer 5'-> 3'
GAPDH	3' end	CATTTCTGGTATGACAACGA	CTTCCTCTTGTGCTCTTGCT
IL-18	3' end	CCTTTAAGGAAATGAATCCTCCT G	CATCTTATTATCATGTCCTGG GAC
Caspase 1	3' end	TGATGCTATTAAGAAAGCCCAC	GAAACATTATCTGGTGTGGA AGAG

Table 8. Designed primers for qPCR.

The reaction setup was prepared on ice under the fume hood (Holten LaminAir). After thawing the reagents, a master mix with the SYBR Green Supermix and nuclease-free water (see Table 9) was prepared for each primer pair (forward and reverse), according to the amount of samples. Then 0.2 µl of forward and reverse primer were added to the reaction mix and mixed thoroughly.

Component	Volume per reaction	Final concentration
Sso Advanced™ Universal SYBR® Green Supermix	5 µl	1x
Forward Primer	0.2 µl	200 nM
Reverse Primer	0.2 µl	200 nM
Nuclease-free H₂O	3.6 µl	
cDNA sample	1 µl	
Total reaction volume	10 µl	

Table 9. Reaction mix for qPCR.

In the 96-well PCR plate, 9 µl of the master mix were distributed to each well. After vortexing the cDNA samples, 1 µl of cDNA was added to each well in triplicates. As a negative control, instead of cDNA, 1 µl nuclease-free H₂O was loaded in triplicates as well. Once all samples were loaded, the PCR plate was sealed with a transparent 'B' seal (Bio-Rad) and vortexed thoroughly. To avoid or remove any air bubbles, the plate was spun down in a centrifuge with the short spin program. The qPCR was run with the StepOne Plus Real-Time PCR System (Applied Biosystems) according to the protocol displayed in Table 10.

Initial Denaturation	Cycles	Denaturation	Annealing/Extension	Melt Curve Analysis
30 sec at 95°C	50	15 sec at 95°C	30sec at 60°C	65-96°C 0.5°C increment 2-5sec/step

Table 10. Thermal cycling protocol for qPCR.

2.9 Statistical Analysis

The software GraphPad Prism v6.01 was used for all statistical analysis and graphic representations.

The analysis of immunohistochemistry was performed with light microscopy. For quantification of IL-18 positive cells, counting was done using an ocular grid with a size of 0.0625 mm² and the 40x magnification objective. Positive cells in the cortical area were counted in 3 grids per sample and afterwards calculated per 1 mm². Data are presented in scatterplots as median with interquartile range (IQR). For multiple comparisons, e.g. comparing pooled RE group, MTLE and MTLE + Enc group to the control group, one-way ANOVA followed by Dunn's test post-hoc was performed. The same procedure was used for comparing individual RE stages to the controls.

The analysis of the amount of microglia and T cells per nodule was performed by generating a scatterplot and calculating the Spearman non-parametric correlation. The variables for microglia were plotted against the horizontal axis and the values for T cells against the vertical axis. A line of best fit, also called trendline, was drawn in order to illustrate the relationship between these two variables.

For qPCR data evaluation, the threshold of the Ct-value was set to 0.3. Furthermore, samples that showed primer dimer formation in the melting curve protocol were excluded from analysis. The results were then normalized with the reference gene GAPDH. Samples from patients suffering from Rasmussen encephalitis were categorized into stage 0, 1 and 2. The mean Ct of each sample triplicate was obtained and for calculation of delta Ct (dCt), the mean Ct of GAPDH was subtracted from the mean Ct of the gene of interest. For optimal representation, delta Ct values were converted into $(1/dCt)^2$ values. For comparison of two groups, the unpaired t-test was used and one-way analysis of variance (ANOVA) with post-hoc Dunn's test

was performed for multiple comparisons. Graphical Data were presented as median with interquartile range (IQR) in scatter plots.

3 Results

3.1 RNA quality measurement

After isolation of RNA from the FFPE samples, we analyzed the RNA quality with the Agilent 2100 Bioanalyzer at the Core Facilities of the Medical University of Vienna. For successful downstream experiments, we analyzed the electropherograms of our samples and decided to use samples with DV200 values above 70%.

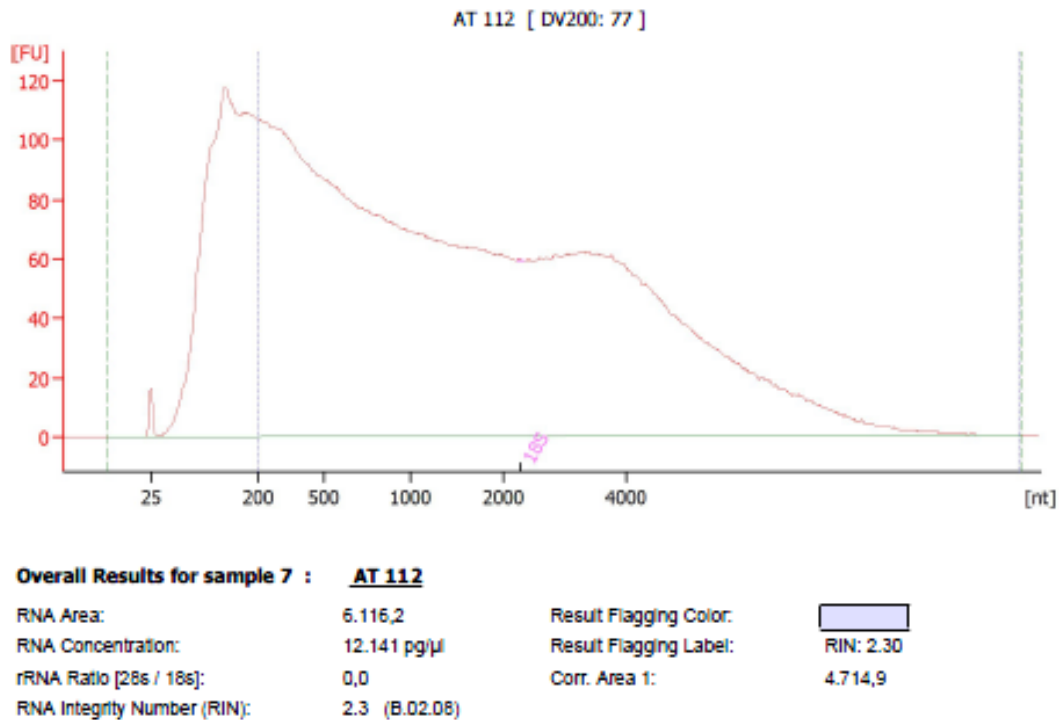
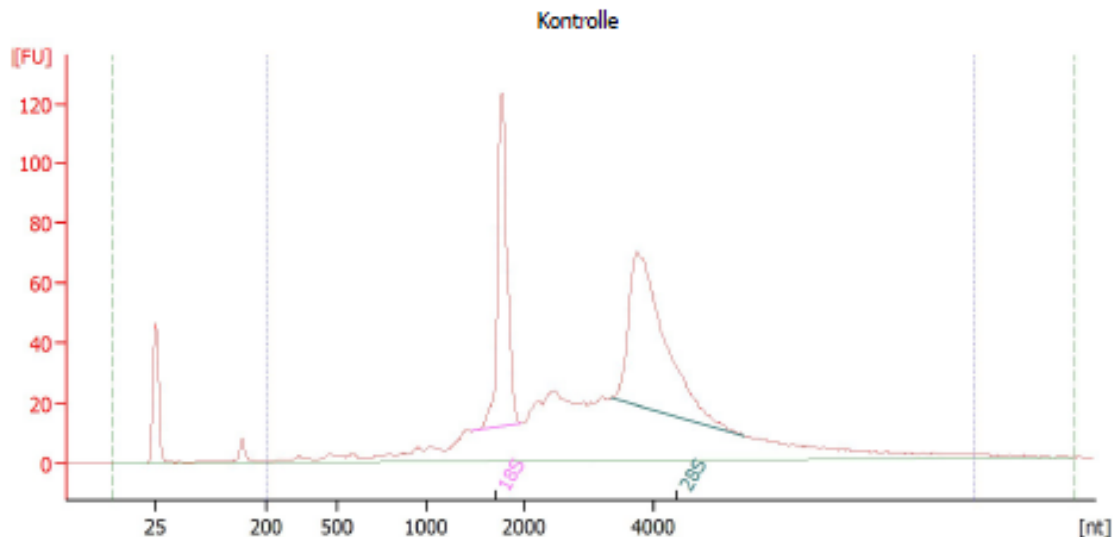


Figure 5. Electropherogram of RNA derived from FFPE tissue. The first peak at 25 nucleotides [nt] shows the marker. The ribosomal peaks are not visible anymore. Around 200 nt there is a big peak that drops early, corresponding to a low number of RNA strands over 200 nt length. nt: nucleotides; FU: fluorescent units

Furthermore, it shows that isolated RNA from FFPE tissue differs from cell culture RNA and is also interpreted differently with different parameters. Samples from cell culture show high quality RNA that is indicated by an rRNA ratio close to 2 and RIN numbers between 8 and 10, with 10 being the maximum value (Figure 6).



Overall Results for sample 1 : Kontrolle

RNA Area:	1.053,4	Result Flagging Color:	
RNA Concentration:	2.066 pg/μl	Result Flagging Label:	RIN:9
rRNA Ratio [28s / 18s]:	1,4	Corr. Area 1:	1.036,6
RNA Integrity Number (RIN):	9 (B.02.08)		

Figure 6. Electropherogram of control RNA analyzed by Agilent 2100 Bioanalyzer.

The first peak around 25 nucleotides [nt] shows the marker. There is a small peak between the marker and 200 nt range, which arises from the RNA isolation process. The ribosomal RNA peaks 18S and 28S can be clearly seen. The baseline between the marker and 18S peak is almost flat and free from small roundish peaks, reflecting small RNA fragments that are degradation products originating from rRNA transcripts. nt: nucleotides; FU: fluorescent units

Altogether, the isolated RNA from our samples resulted in satisfactory concentration levels and adequately long RNA fragments. Therefore, the RNA was good enough to use for future experiments, such as real-time qPCR.

3.2 Analysis of Interleukin-18 and Caspase 1 mRNA levels in Rasmussen encephalitis and Mesial temporal lobe epilepsy

In this study, we investigated the presence of IL-18 and caspase 1 that are part of the inflammasome, in different stages of RE as well as in MTLE samples. Because the most interesting pathological events, in terms of inflammation, occur in RE cases staged 0, 1 and 2, we only used these stages. For the analysis of RE samples, only the RNA of the cortical grey matter was isolated and compared to the control samples, which also composed of RNA from the cortex. For MTLE and MTLE + Enc cases, the RNA of the hippocampus was used. The results for the RE cases were

pooled in one group and compared to the control group. Additionally, we compared other epileptic disorders such as MTLE and MTLE + Enc to the control group.

3.2.1 Elevated expression of Caspase 1 in intermediate stage of RE

We examined the expression levels of caspase 1 and the pooled RE cases as well as the MTLE and MTLE + Enc group were compared to the control group (Figure 7). The mRNA levels of caspase 1 appear to be significantly higher in the pooled RE group as well as the MTLE and MTLE + Enc group compared to the control group (Figure 7A). When we compared the individual stages to the control group, the graph showed a continuous rise, but statistics demonstrated that caspase 1 is significantly higher only in stage 2 (Figure 7B). Interestingly, compared to the control group, the MTLE group also showed a significant increase of caspase 1. In this statistical evaluation, the MTLE + Enc group showed no difference, which can be explained by the low number of samples for this group and increased number of tests (post-hoc correction).

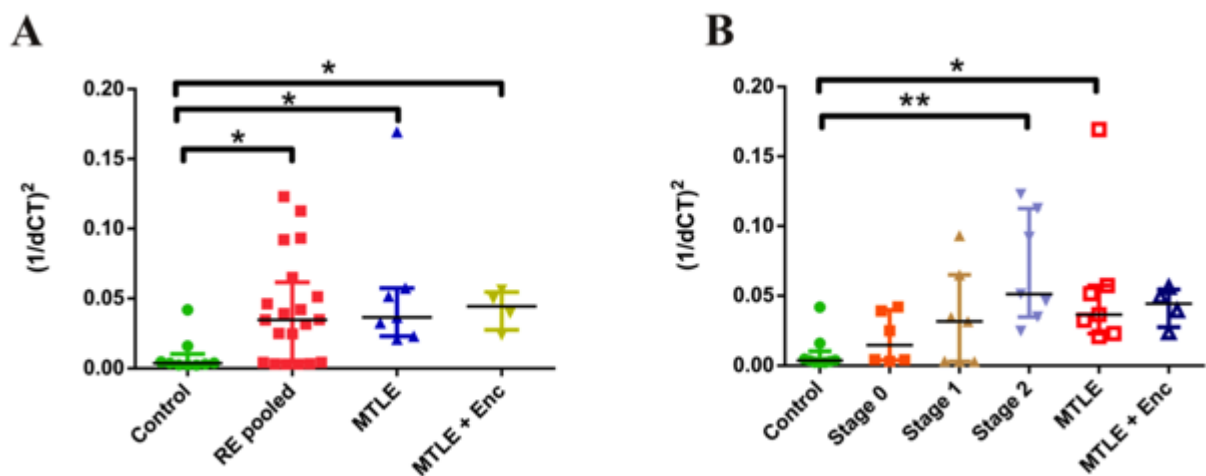


Figure 7. Statistical evaluation of caspase 1 mRNA levels. One-way ANOVA with post-hoc Dunn's test was performed for multiple comparisons. **A:** Pooled RE cases (n = 20), MTLE cases (n = 7) and MTLE + Enc (n = 4) were compared to the control group (n = 9) and showed elevated caspase 1 values. **B:** The individual stages (Stage 0: n = 6; Stage 1: n = 7; Stage 2: n = 7) and the MTLE groups were compared to the control group. Statistical analysis revealed significantly higher caspase 1 levels in stage 2, but also in the MTLE group. (* p < 0.05; ** p < 0.01) Data is shown as median \pm IQR.

3.2.2 Interleukin-18 expression increased in early stage of RE

The statistical evaluation revealed that the mRNA levels of IL-18 were significantly higher in RE patients than in the control group. Furthermore, comparison of the

MTLE groups to the control group showed no significant increase of IL-18 (Figure 8A). The stages of RE were also analyzed individually and compared to the control group. Stage 1 presented a significant increase of IL-18 in comparison to the controls, whereas the other stages displayed increased levels, yet no significant differences were observed. In stage 2 we observed a decrease in the expression levels compared to stage 1, but the results were not significant. The results of MTLE and MTLE + Enc revealed again no significant upregulation compared to the control group (Figure 8B), however there seems to be a trend towards higher levels of IL-18 in MTLE + Enc compared to MTLE.

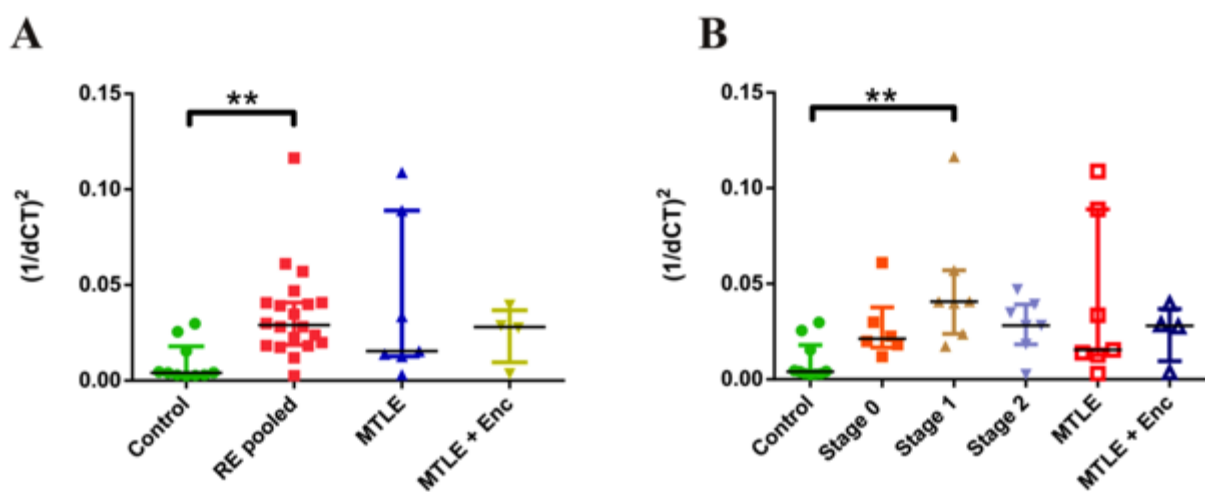


Figure 8. Statistical evaluation of IL-18 mRNA levels. One-way ANOVA with post-hoc Dunn's test was performed for multiple comparisons. **A:** mRNA levels of IL-18 in RE (n = 20), MTLE (n = 7) and MTLE + Enc (n = 4) were compared to the control group (n = 10). The pooled RE group shows a significant increase of IL-18 levels, whereas in MTLE and MTLE + Enc IL-18 is not elevated. **B:** The stages of RE are compared separately to the control. In stage 1 (n = 7) IL18 is increased, while in stage 0 (n = 6) and stage 2 (n = 7) no significance was found. Statistics confirmed that there is no upregulation in MTLE and MTLE + Enc. (** p < 0.01) Data is shown as median \pm IQR.

3.3 Qualitative and quantitative immunohistochemical evaluation

3.3.1 Presence of Interleukin-18 in Rasmussen encephalitis and Mesial temporal lobe epilepsy

Another important aim in this study was to assess the presence of the cytokine IL-18 on the protein level, determine its location and also quantify it in the different stages of RE and MTLE groups. Therefore, all samples of the control group, RE group, MTLE and MTLE + Enc group were stained for IL-18 and positive cells were counted

by light microscopy. In the control and RE cases, we counted positive cells in the cortex, while in the MTLE groups, the region of the hippocampus was counted, since it is the affected region of the disease.

In controls and RE cases, IL-18 was found in microglial cells as well as neurons throughout the cortex and endothelial cells. IL-18 was detected in the soma and the cell projections of microglia. Furthermore, IL-18 positive microglia were found to be concentrated in nodules of various sizes in RE (Figure 9). The smallest nodules consisted of only 3-4 cells and were found in the grey matter of stage 0 to stage 2 samples and in some cases in the underlying white matter (Fig. 9A). In stage 1 samples we also found larger nodules with up to 10-30 microglial cells. These nodules also contained T cells and often were found surrounding individual neurons. We also discovered that the small nodules consisting of 3-4 cells already presented caspase 1 positive microglia (Figure 10) and large nodules with 10 or more microglia expressed caspase 1 as well. Compared to stage 1, in stage 2 we could observe even more IL-18 positive microglia in the cortex. Positive microglia were also present in lesions. In the MTLE cases we found IL-18 positive microglia and neurons in the hippocampus, namely in the CA and dentate gyrus areas.

Preliminary work of my colleague showed no presence of IL-1 β in small nodules, only large nodules were IL-1 β positive. Generally, only very few IL-1 β positive cells were sporadically distributed in the RE samples.

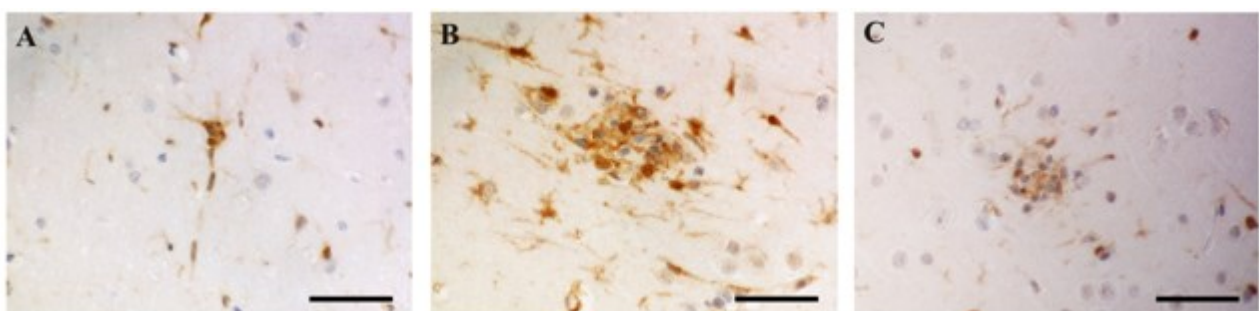


Figure 9. Immunohistochemical staining for IL-18 in RE. A: Very small nodule with microglia positive for IL-18 in RE. **B and C:** Bigger nodule with IL-18 positive microglia. Scale bar: 50 μ m

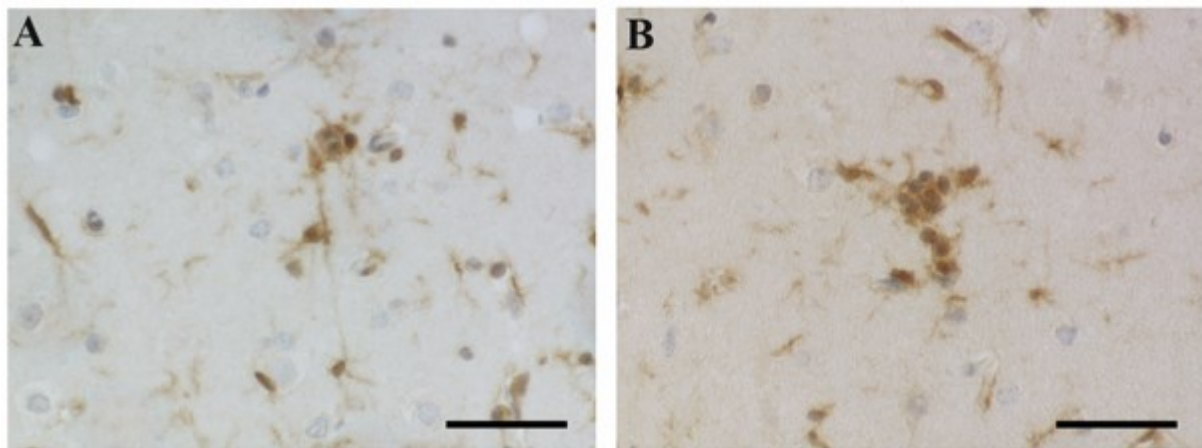


Figure 10. Immunohistochemical staining for caspase 1 in RE. Small nodules also exhibited caspase 1 positivity in RE samples. Scale bar: 50 μ m

In addition, the presence of IL-18 in nodules was confirmed by confocal laser microscopy of fluorescent immunohistochemical double stainings for IL-18 and CD68, a marker for microglia. The double staining in the RE sample showed once again that small nodules already produce the cytokine (Figure 11).

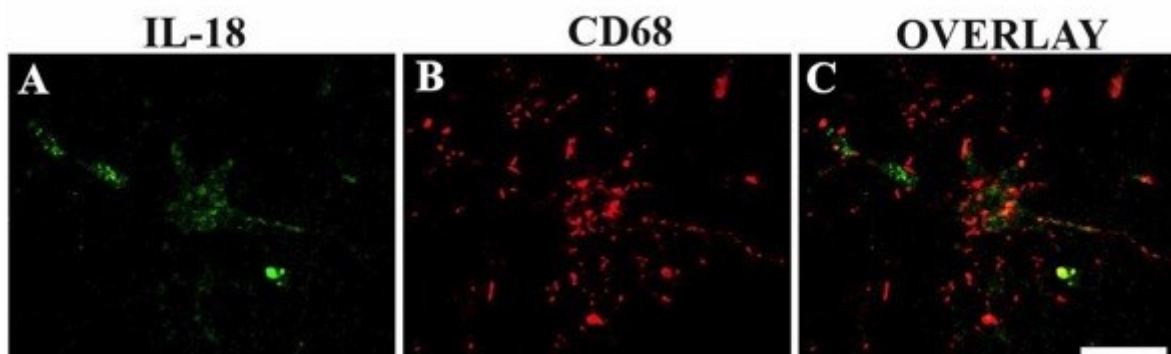


Figure 11. Fluorescent IHC for IL-18 and CD68 in RE. **A:** IL-18 is labeled in green (Cy2). **B:** CD68 is labeled in red (Cy3). **C:** The overlay of fluorophores showed that IL-18 colocalizes with CD68. Scale bar: 20 μ m

The quantitative evaluation of IL-18 was performed with the help of a morphometric grid and revealed that the values for IL-18 of the pooled RE group was significantly higher than in the control group. Once more, we checked if other epileptic disorders (MTLE and MTLE + Enc) also differ from the control group. However, results show that there was no significant difference found (Figure 12A). The analysis of the individual RE stages exposed a higher number of IL-18 positive cells in stage 1 and 2. Once again, values obtained from MTLE and MTLE + Enc were not significantly elevated (Figure 12B).

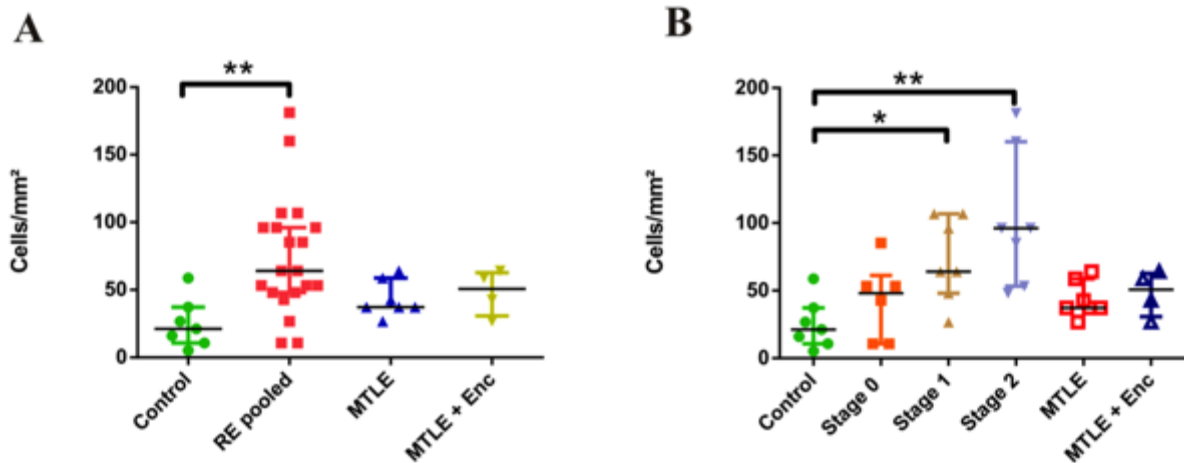


Figure 12. Statistical analysis of the quantification of IL-18 positive cells. **A:** Values of IL-18 positive cells per mm² pooled RE cases (n = 20), MTLE (n = 7) and MTLE + Enc (n = 4) were compared to the control group (n = 7). **B:** Individual stages of RE (Stage 0: n = 6; Stage 1: n = 7; Stage 2: n = 7) compared to the control group showed a significant increase of IL-18 positive cells in stage 1 and 2. (* p < 0.05; ** p < 0.01) One-way ANOVA with post-hoc Dunn's test was performed for multiple comparisons. Data is shown as median ± IQR.

3.3.2 Microglial nodules in Rasmussen encephalitis and viral encephalitis

3.3.2.1 Distinction of microglia and macrophages in nodules

To ensure that the nodules in the cortex are composed of activated microglia and not peripheral macrophages, we made use of the new microglial marker Tmem119. It serves as a reliable microglial marker that is solely expressed on ramified and amoeboid microglia, with no expression on peripheral (infiltrating) macrophages (Sato et al., 2015). Therefore, fluorescent IHC stainings for Iba1 and Tmem119 were performed on RE and viral encephalitis samples and examined with the confocal laser microscope. Viral encephalitis samples were used for comparison to RE samples and to show that microglial nodules are a characteristic hallmark these two diseases have in common. As expected, it was found that the nodules in samples of RE and viral encephalitis solely consisted of Tmem119 positive resident microglia (Figure 13).

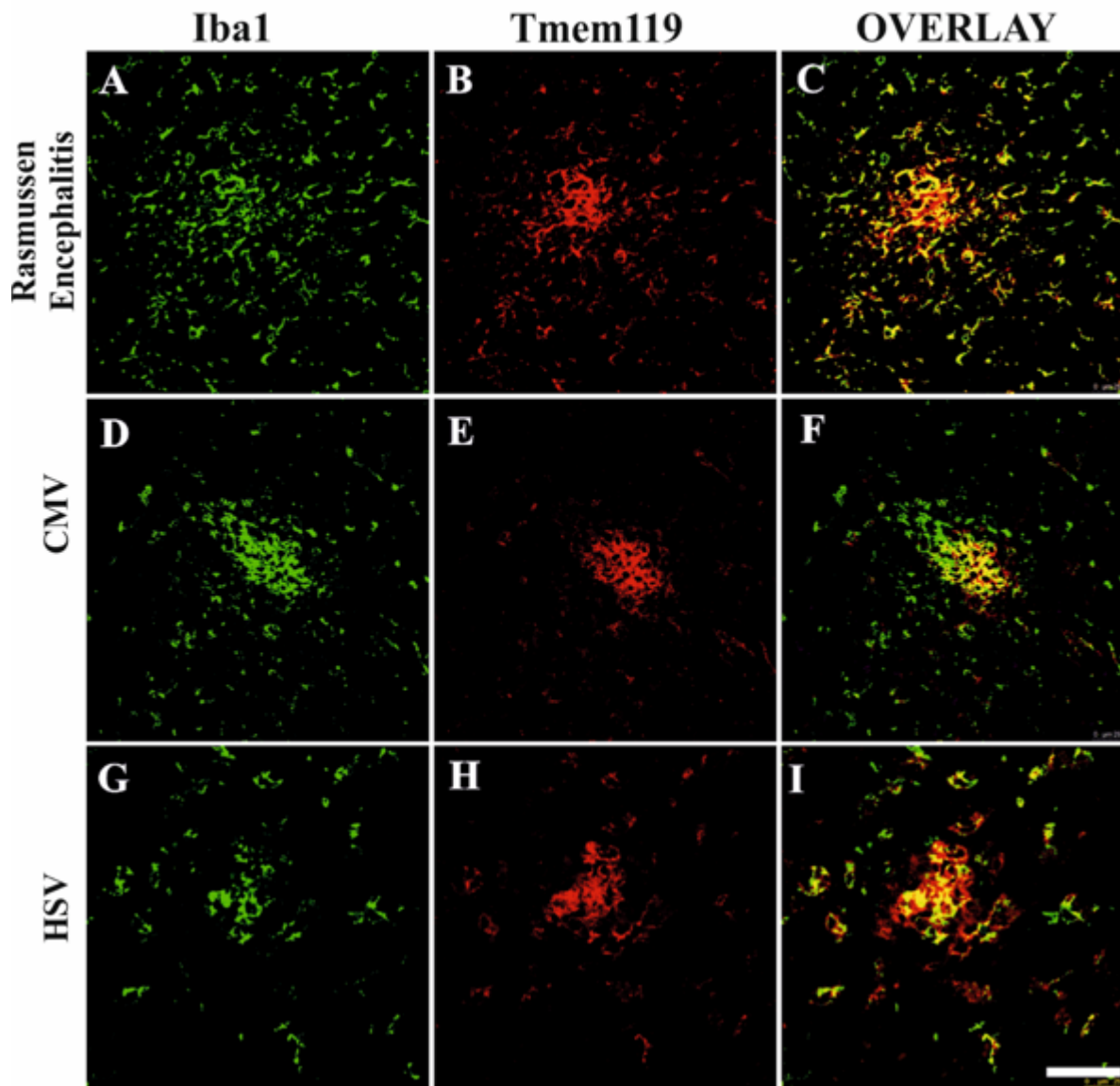


Figure 13. Fluorescent IHC for Iba1 and Tmem119 in RE and viral encephalitis. A, D, G: Iba1 is labeled in green (Cy2). **B, E, H:** Tmem119 is labeled in red (Cy3). **C, F, I:** Overlay of fluorophores showed the Iba1⁺Tmem119⁺ positive nodules. Scale bar: 50 μ m

3.3.2.2 Relationship of microglia and T cells in microglial nodules in Rasmussen encephalitis

The second approach was the analysis of microglial nodules in RE and to find out if there is an association between the size of the nodules and T cell infiltration. To this end, double stainings for microglia (Iba1) and T cells (CD3, CD8) were performed on 14 RE samples selected independently of the stage. The amounts of T cells and microglia per nodule were determined and statistically interpreted in RE cases.

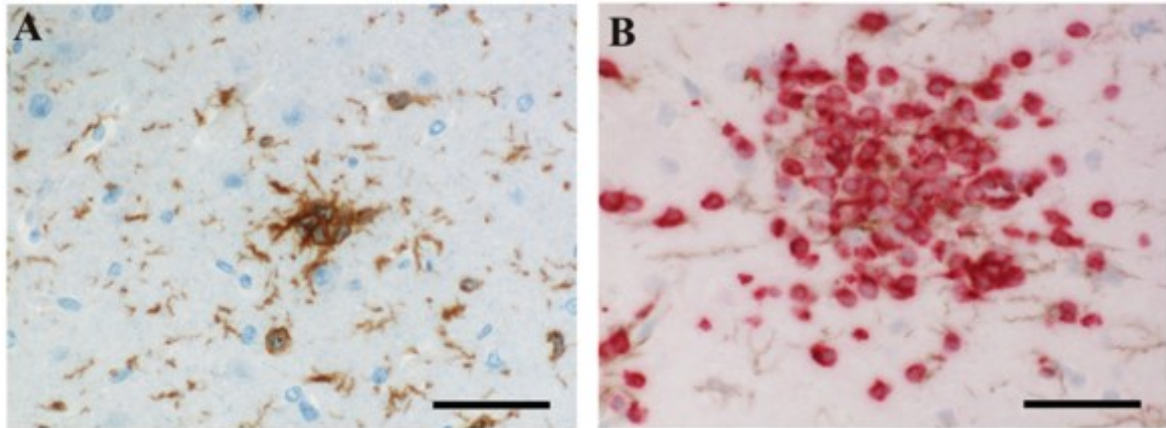


Figure 14. Immunohistochemical double stainings for Iba1 and CD3/CD8 in RE cases. A: Small nodule without T cell infiltration. **B:** Bigger nodule of microglia (brown) with massive T cell infiltration (red). Scale bar: 50 μ m

Investigation of the microglial nodules in RE showed that most of them were composed of microglia as well as T cells (Figure 14). Small nodules were found to contain no T cells, while large nodules exhibited the presence of T cells. Besides the presence of T cells in nodules, they were also found spread throughout the cortex and in perivascular regions.

As described earlier, viral encephalitis is a striking example for the presence of microglial nodules. Therefore, we also examined samples from viral encephalitis cases under the microscope and looked for the characteristic nodules. Figure 15 shows different cases of viral encephalitis containing microglial nodules in the cortical grey matter, which presented T cell infiltration with a varying extent. The T cells in these cases were mainly of the CD8 phenotype. Additionally, nodules were also found in the underlying white matter.

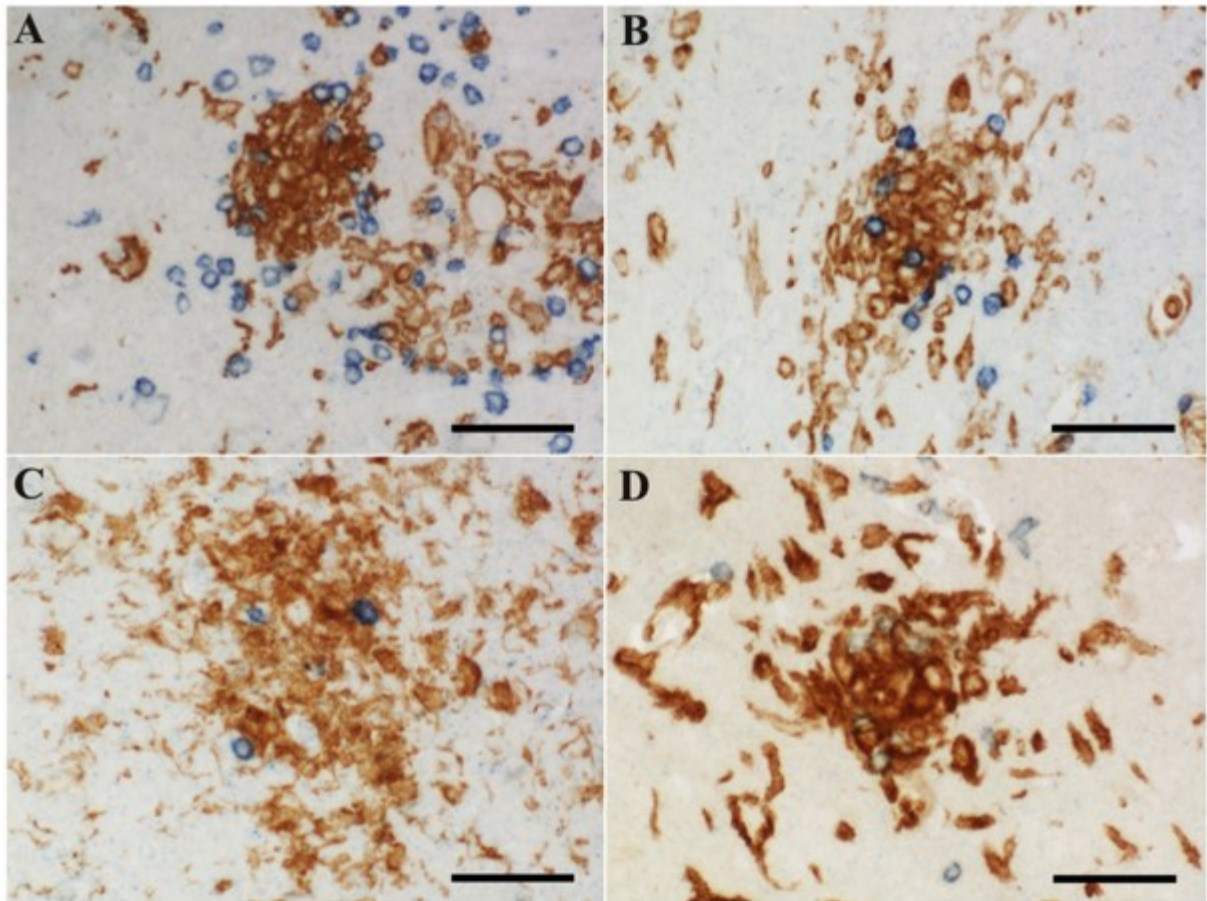


Figure 15. Different viral encephalitis cases presenting microglial nodules in the cortex. A: Microglial nodule (brown) with slight T cell infiltration (blue) in the cortex of a CMV brain. **B:** Sample of TBE presenting a microglial nodule. **C:** HSVE case with microglial nodule. **D:** Nodule with very few T cells in a PML case. Scale bar: 50 μ m

In order to find out if the formation and activation of microglial nodules precedes T cell infiltration, we quantified microglia and T cells in nodules. The results exposed that with increasing microglia the amount of T cells also increased, resulting in a positive correlation of these two values (Figure 16). Smaller nodules of 3-4 microglia therefore contain often only very few T cells or no T cells, in contrast to big nodules that always contain T cells.

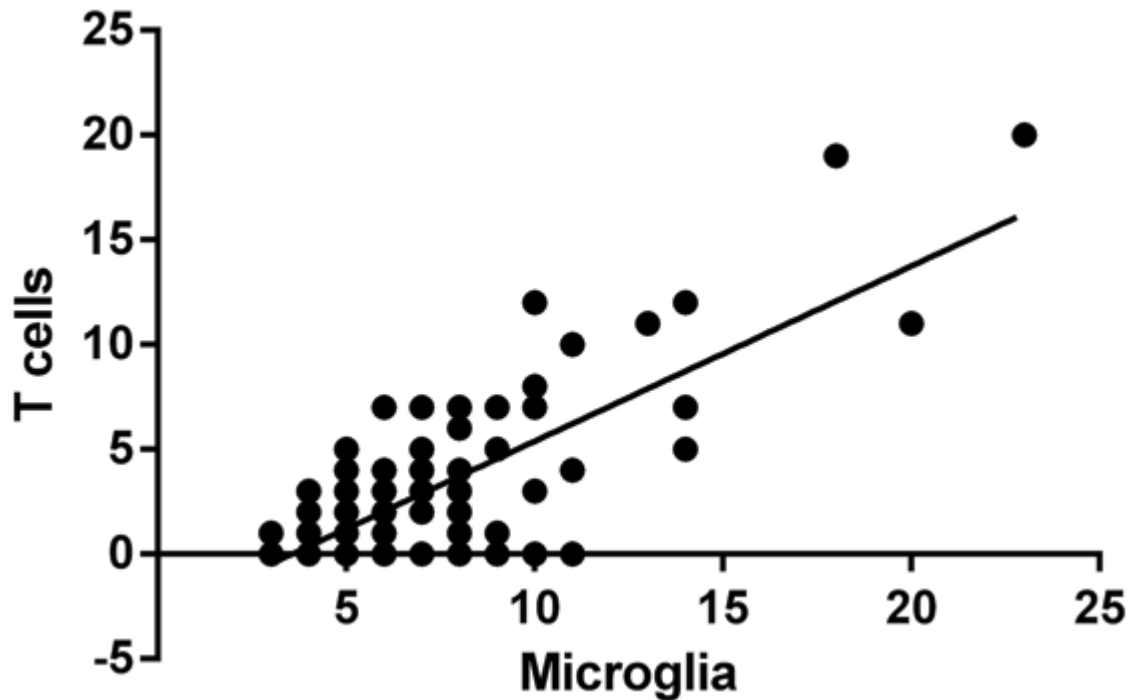


Figure 16. Correlation diagram of microglia and T cells. The x-axis gives the amount of microglia counted per nodule, the y-axis gives the amount of T cells per nodule. A nodule was defined by consisting of a minimum of 3 microglia. By drawing a trendline, a positive correlation between microglia and T cells was revealed (Spearman $r = 0.4989$; $p < 0.0001$).

3.3.2.3 Detection of P-Stat1 positive cells in microglial nodules

P-Stat1 is a transcription factor that is upregulated in the nucleus as result of IFN signaling. Here, we examined if P-Stat1 presence was associated with the presence of T cells in microglial nodules. Stainings for P-Stat1 showed presence in the nucleus of neurons and microglia, prevalently in microglial nodules of bigger size. In small nodules of 3-4 microglia we could not detect the presence of P-Stat1. In larger neurons, P-Stat1 however was present in microglial cells, in neurons, T cells and possibly astrocytes. Besides the positive nodules, we also observed P-Stat1 positive cells with morphology of T cells irregularly distributed throughout the cortex. Surprisingly, some samples exhibited P-Stat1 positive cell projections, that might be axons, but they were not further investigated (Figure 17C). Viral encephalitis cases were also inspected and showed P-Stat1 positive nodules (Figure 17).

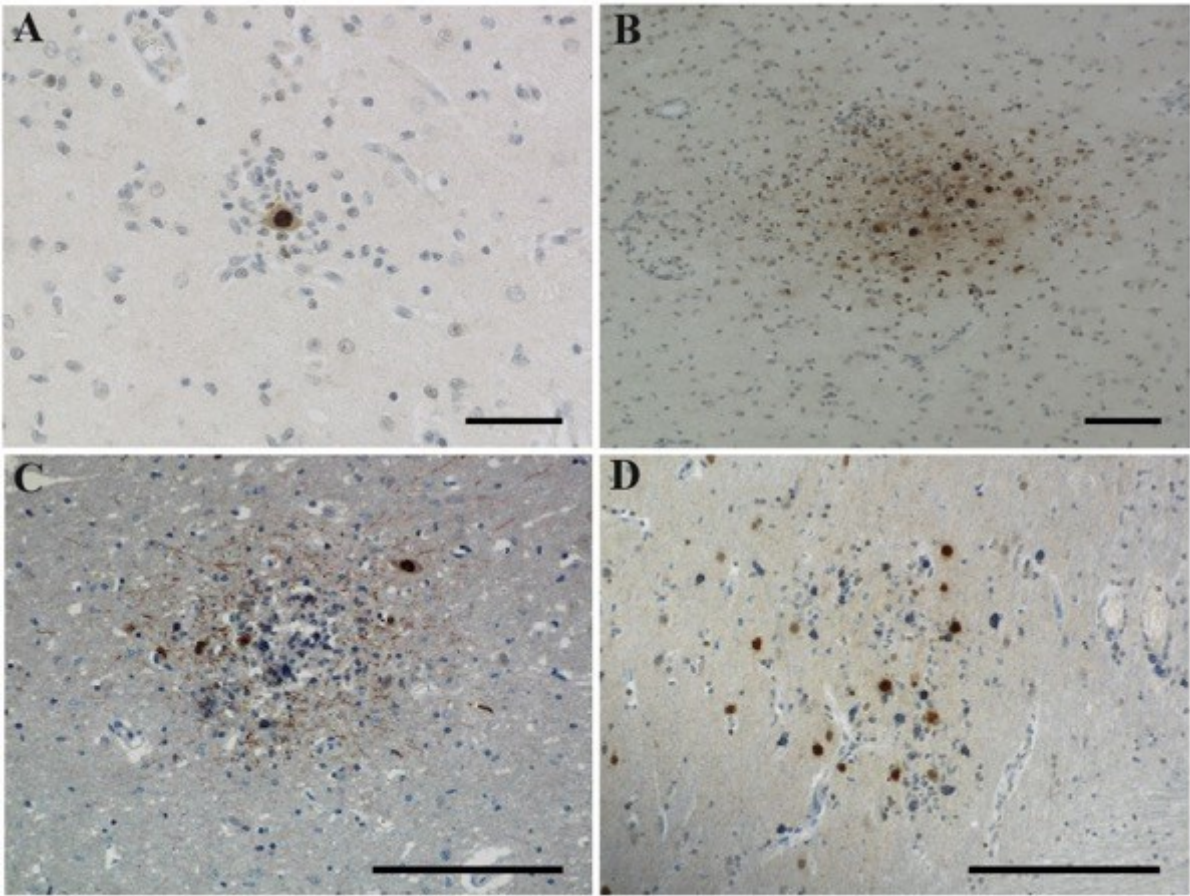


Figure 17. IHC P-Stat1 with counterstaining. A, B: Stat1 (brown) accumulated in microglial nodules in RE samples. **A:** Presence of P-Stat1 in the nucleus of a neuron encircled by microglia. **B:** P-Stat1 positive nuclei of microglia and neurons. **C:** TBE case with a positive nodule. **D:** CMV sample with P-Stat1 positive cells distributed in and around a nodule, near blood vessels. Scale bar: A: 50 μ m; B: 100 μ m; C, D: 200 μ m

4 Discussion

The aim of this study was to investigate microglial nodules and the role of the inflammatory mediators in these nodules. In this work, we focused on RE and attempted to give an insight into the inflammatory pathways and microglial nodule formation.

The analysis of IL-18 and caspase 1 transcripts as part of the inflammasome was performed by qPCR of FFPE samples. RNA extraction from FFPE tissue remains a big challenge. FFPE is an excellent method for long-term preservation of most pathological specimens and these samples provide a precious resource for molecular studies (Lin et al., 2009). The reagent formaldehyde leads to cross-linking of nucleic acids and proteins, and causes nucleic acids fragmentation due to fixation process conditions (Gilbert et al., 2007). Hence, it is very difficult to extract RNA or DNA, and amplify high molecular weight DNA (Lin et al., 2009). The cross-linking not only complicates isolation of nucleic acids, but is also blocking PCR amplification (Gilbert et al., 2007).

Due to the well-known problems with RNA extraction from FFPE tissue, our RNA samples had to pass several previously described quality criteria to be used in further downstream applications. We first started with the quality assessment of our RNA samples. The electropherograms of our samples showed the presence of small RNA fragments, indicated by changes in the shape of the curve, which results in low rRNA ratios and low RIN numbers. Therefore, we needed to use different parameters for assessing the RNA quality. The amplitude and length of the resulting plateau are important parameters for RNA quality from FFPE tissue. An early drop of the plateau suggests a low number of long RNA fragments. Another relevant parameter we used is the DV200 number.

After successful RNA isolation, we could show that the gene expression of caspase 1, as component of the inflammasome, was increased in the RE group compared to the controls. Furthermore, caspase 1 was significantly upregulated in stage 2 compared to the controls. In stage 1, the caspase 1 expression was not significantly increased, but we found higher values compared to the control group. Interestingly, caspase 1 is also upregulated in the MTLE groups, even though IL-18 was not upregulated, which can be explained by the notion that caspase 1 also cleaves many other substrates such as IL-1 β (Jha et al., 2010). There are various proteomics studies that suggest diverse substrate specificities for caspase 1. In the MTLE

samples we did not detect microglial nodules, thus we think that these nodules play a major role in the inflammatory response in RE.

Since IL-18 is a pro-inflammatory cytokine and chronic grey matter inflammation is present in RE, we hypothesized that IL-18 is upregulated in RE compared to the controls. Our results revealed that the mRNA levels of IL-18 are significantly higher in the RE group than in the control group. When we compared IL-18 levels in the individual RE stages, we found a significant increase in stage 1 of RE compared to the control group. The values for stage 0 and stage 2 were slightly higher than in the control group, but no significant differences were found. Our findings aroused speculation that IL-18 might be an important player in the early inflammation stage of RE and decreases in later stages. Consistent with our expectations, the MTLE and MTLE + Enc groups showed no significant increase in IL-18 mRNA levels, but the MTLE + Enc group had marginally higher levels in comparison with the MTLE group, that could be probably explained by the presence of viral encephalitis in the past. Moreover, seizures can also trigger mild inflammatory reactions.

IHC stainings for IL-18 were performed to analyze the inflammasome components on the protein level. The results revealed that the cytokine was already produced in stage 0 cases of RE, concentrated in microglial nodules in the cortex. Moreover, the small nodules were also caspase 1 positive, which seems plausible since the enzyme is needed for the processing of IL-18. It is important to mention that the used antibody detects the cleaved as well as the precursor form of IL-18, therefore it was not possible to distinguish between the active and inactive protein. However, as IL-18 and caspase 1 were both expressed in the small nodules, and caspase 1 is required for processing of active IL-18 to be secreted, it might indicate that already small nodules secrete this proinflammatory cytokine. By contrast, IL-1 β was only observed in big nodules. The production of IL-1 β may need an additional activation signal that might be provided later in the course of disease, possibly by T cells. In addition, we performed cell countings under the light microscope and detected elevated production of IL-18 in RE compared to the controls, which fits to our data collected from qPCR. In the individual stages, we could already observe a rise in stage 0 compared to the control group, but significant differences were only found in stage 1 and stage 2. These findings suggest that microglial inflammasome activation already starts in the earliest stage of disease and leads to the activation of further inflammatory signaling pathways.

For the characterization of the nodules, we performed numerous IHC stainings and first confirmed the presence of microglial nodules in RE samples. Smaller nodules consisting of 3-4 microglia were already found in RE stage 0 cases. Immunohistochemical stainings of RE cases also showed that T cells in the nodules were mainly CD8 positive cells, agreeing with the previous findings from Bien et al. who showed that lymphocytic infiltrates consisted mainly of CD3⁺CD8⁺ T cells (Bien et al., 2002a).

Another important question we were interested in was if microglial activation precedes T cell infiltration. We could show that the amount of microglia and T cells in nodules correlated positively. The smallest nodules with only 3 microglial cells exhibited no T cells, while bigger nodules contain T cells. A recent study showed that the expression of genes related to several chemokines is upregulated in RE (Owens et al., 2013), but a question that still needs to be resolved is if these nodules might be involved in this.

Moreover, the presence of IFNs in RE was investigated by IHC stainings for P-Stat1. Our results demonstrated that P-Stat1 was present in microglial cells, but also neurons and probably astrocytes. P-Stat1 positive neurons encircled by microglia could also be observed. In the smaller nodules of 3-4 microglia we could not detect P-Stat1. Our results therefore suggest that IFN signaling is induced by T cells in larger nodules. In line with this finding, unpublished microarray data from my colleague revealed increased expression of IFN genes in stage 1 cases. Type I interferons can induce the inflammasome activation by enhancing the expression of inflammasome components (Kim et al., 2016).

To summarize, we were able to show that microglial inflammasome activation already occurs in stage 0 of RE because the expression of inflammasome genes such as caspase 1 and IL-18 is increased. IHC stainings confirmed that IL-18 is produced already in the small nodules of RE samples and elevated in RE compared to the control group, whereas preceding work by my colleague showed that IL-1 β gene expression is increased later in the course of disease. Furthermore, the microglial activation seems neither to be provoked by T cells nor IFNs, as we could not detect them in the small nodules. Consequently, the inflammasome activation is either triggered by DAMPs or PAMPs.

These observations suggest that microglial nodules generate an inflammatory milieu probably provoked by IL-18. In the course of disease, T cells might get attracted by

the microglial production of chemokines which is induced by IL-18 (Felderhoff-Mueser et al., 2005). Chemokines are necessary for the recruitment of T cells and their localization still needs to be elucidated in RE. Interestingly, numerous studies reported the ability of IFNs to regulate the synthesis of chemokines (Rauch et al., 2013). Moreover, IL-18 can enhance the production of pro-inflammatory IL-1 β and IFN γ , its involvement possibly leads to a vicious cycle, where inflammatory reactions contribute to various aspects of neurodegeneration (Businaro et al., 2016).

Future investigations will be important to give more insight into the inflammatory signaling pathways of RE. According to literature, neuronal damage in RE is starting to emerge in stage 1 (Pardo et al., 2004) and we could not detect any neuronal damage in our cases of stage 0 either. However, it might be that there is some minor change in the neighborhood of the small nodules that we overlooked. Thus, it would be wise to perform fluorescence double stainings with Iba1 and amyloid precursor protein (APP), which marks axonal degeneration. Additional experiments on this work could be to investigate the location and presence of interferons. We did not show the colocalization of caspase 1 and IL-18, therefore double labelings could be performed to verify the presence of these components in small nodules.

Our results might lead to the suspicion of a viral infection, therefore the search for a rare pathogen still needs to be continued. Another interesting question is the characterization of microglial nodules in comparison to microglia in the surrounding brain parenchyma. Lastly, the examination of the inflammasomes in CNS pathologies appears to be an important step for the finding of therapeutic targets. To date, various advances have been made in the discovery of exogenous compounds that may block or inhibit inflammasome signaling pathways. However, most of them are still in the early stages of development (Song et al., 2017; White et al., 2017).

5 List of Abbreviations

×g	Gravitational acceleration
Ab	Antibody
a.d.	Aqua destillata
AEDs	Antiepileptic drugs
ANOVA	Analysis of variance
AP	Alkaline phosphatase
AP1	Activator protein 1
APP	Amyloid precursor protein
BBB	Blood-brain barrier
CA1	Cornu ammonis area 1
cDNA	Complementary deoxyribonucleic acid
CMV	Cytomegalovirus
CNS	Central nervous system
COX	Cyclooxygenase
CSA	Catalyzed signal amplification
CSF	Cerebrospinal fluid
Cy	Cyanine
DAB	3,3'-Diaminobenzidine
DAMP	Damage-associated molecular pattern
dCt	Delta cycle threshold
DNA	Deoxyribonucleic acid
EAE	Experimental autoimmune encephalomyelitis
EBV	Epstein-Barr virus
EDTA	Ethylenediaminetetraacetic acid
Enc	Encephalitis
EtOH	Ethanol
FCS	Fetal calf serum
FFPE	Formalin-fixed paraffin-embedded
g	Gram(s)
GABA	Gamma aminobutyric acid
GAPDH	Glyceraldehyde 3-phosphate dehydrogenase
H ₂ O ₂	Hydrogen peroxide
HCl	Hydrochloric acid
HE	Hematoxylin and eosin
HMGB1	High-mobility group box 1
HIV	Human immunodeficiency virus
HS	Hippocampal sclerosis
HSE	Herpes simplex encephalitis
HSV	Herpes simplex virus
Iba1	Ionized calcium-binding adapter molecule 1
IFNAR	Interferon-alpha/beta receptor
IFNGR	Interferon-gamma receptor
IFN	Interferon
IHC	Immunohistochemistry
IL-18	Interleukin-18
IL-1 β	Interleukin-1 beta
IL	Interleukin
IQR	Interquartile range
Jak	Janus kinase
JCV	John Cunningham virus

KHCO ₃	Potassium bicarbonate
L	Liter(s)
LPS	Lipopolysaccharide
M	Molar
MAPK	Mitogen-activated protein kinase
mg	Milligram(s)
ml	Milliliter(s)
mM	Millimolar
MgSO ₄	Magnesium sulfate
MRI	Magnetic resonance imaging
mRNA	Messenger ribonucleic acid
MS	Multiple sclerosis
MTLE	Mesial temporal lobe epilepsy
NaCl	Sodium chloride
NaH ₂ PO ₄	Monosodium phosphate
Na ₂ HPO ₄	Disodium phosphate
NaNO ₂	Sodium nitrite
ng	Nanogram(s)
NeuN	Neuronal nuclear antigen
NFκB	Nuclear factor kappa B
NLR	Nucleotide binding and oligomerization domain-like receptor
NOD	Nucleotide binding and oligomerization domain
PAMP	Pathogen-associated molecular pattern
PI3K	Phosphoinositide 3-kinase
PLA ₂	Phospholipases A ₂
PBS	Phosphate buffered saline
PML	Progressive multifocal leukoencephalopathy
PRR	Pattern recognition receptor
qPCR	Quantitative polymerase chain reaction
RE	Rasmussen encephalitis
RIN	RNA integrity number
ROS	Reactive oxygen species
rpm	Revolutions per minute
rRNA	Ribosomal ribonucleic acid
SDS	Sodium dodecyl sulphate
SE	Status epilepticus
Stat	Signal transducers and activators of transcription
TBI	Traumatic brain injury
TBS	Tris buffered saline
TBEV	Tick-borne encephalitis virus
TGF-β	Transforming growth factor
TLE	Temporal lobe epilepsy
TLR	Toll-like receptor
Tmem119	Transmembrane protein 119
TNFα	Tumor necrosis factor alpha
TNF	Tumor necrosis factor
ZNS	Zentralnervensystem
μg	Microgram(s)
μl	Microliter(s)

6 References

- Agostini, L., F. Martinon, K. Burns, M.F. McDermott, P.N. Hawkins, and J. Tschopp. 2004. NALP3 Forms an IL-1 β -Processing Inflammasome with Increased Activity in Muckle-Wells Autoinflammatory Disorder. *Immunity*. 20:319-325.
- Alboni, S., D. Cervia, S. Sugama, and B. Conti. 2010. Interleukin 18 in the CNS. *J Neuroinflammation*. 7:9.
- Antonelli, M., and I. Kushner. 2017. It's time to redefine inflammation. *Faseb J*. 31:1787-1791.
- Arribas, J.R., G.A. Storch, D.B. Clifford, and A.C. Tselis. 1996. Cytomegalovirus encephalitis. *Ann Intern Med*. 125:577-587.
- Banati, R.B., G.W. Goerres, R. Myers, R.N. Gunn, F.E. Turkheimer, G.W. Kreutzberg, D.J. Brooks, T. Jones, and J.S. Duncan. 1999. [C-11](R)-PK11195 positron emission tomography imaging of activated microglia in vivo in Rasmussen's encephalitis. *Neurology*. 53:2199-2203.
- Bauer, J., C.E. Elger, V.H. Hans, J. Schramm, H. Urbach, H. Lassmann, and C.G. Bien. 2007. Astrocytes are a specific immunological target in Rasmussen's encephalitis. *Ann Neurol*. 62:67-80.
- Becker, K. 2006. Innate and adaptive immune responses in CNS disease. *Clinical Neuroscience Research*. 6:227-236.
- Berger, J.R. 2007. Progressive multifocal leukoencephalopathy. In *Handbook of Clinical Neurology*. Vol. 85. Elsevier. 169-183.
- Bertke, A.S., A. Patel, Y. Imai, K. Apakupakul, T.P. Margolis, and P.R. Krause. 2009. Latency-associated transcript (LAT) exon 1 controls herpes simplex virus species-specific phenotypes: reactivation in the guinea pig genital model and neuron subtype-specific latent expression of LAT. *J Virol*. 83:10007-10015.
- Bien, C.G., J. Bauer, T.L. Deckwerth, H. Wiendl, M. Deckert, O.D. Wiestler, J. Schramm, C.E. Elger, and H. Lassmann. 2002a. Destruction of neurons by cytotoxic T cells: a new pathogenic mechanism in Rasmussen's encephalitis. *Ann Neurol*. 51:311-318.
- Bien, C.G., T. Granata, C. Antozzi, J.H. Cross, O. Dulac, M. Kurthen, H. Lassmann, R. Mantegazza, J.G. Villemure, R. Spreafico, and C.E. Elger. 2005. Pathogenesis, diagnosis and treatment of Rasmussen encephalitis: a European consensus statement. *Brain*. 128:454-471.
- Bien, C.G., H. Tiemeier, R. Sassen, S. Kuczaty, H. Urbach, M. von Lehe, A.J. Becker, T. Bast, P. Herkenrath, M. Karenfort, B. Kruse, G. Kurlemann, S. Rona, S. Schubert-Bast, S. Vieker, S. Vlaho, B. Wilken, and C.E. Elger. 2013. Rasmussen encephalitis: incidence and course under randomized therapy with tacrolimus or intravenous immunoglobulins. *Epilepsia*. 54:543-550.
- Bien, C.G., H. Urbach, M. Deckert, J. Schramm, O.D. Wiestler, H. Lassmann, and C.E. Elger. 2002b. Diagnosis and staging of Rasmussen's encephalitis by serial MRI and histopathology. *Neurology*. 58:250-257.
- Bossù, P., A. Ciaramella, F. Salani, D. Vanni, I. Palladino, C. Caltagirone, and G. Scapigliati. 2010. Interleukin-18, From Neuroinflammation to Alzheimer's Disease. 4213-4224 pp.
- Businaro, R., M. Corsi, G. Azzara, T. Di Raimo, G. Laviola, E. Romano, L. Ricci, M. Maccarrone, E. Aronica, A. Fuso, and S. Ricci. 2016. Interleukin-18 modulation in autism spectrum disorders. *J Neuroinflammation*. 13:2.
- Cherry, J.D., J.A. Olschowka, and M.K. O'Banion. 2014. Neuroinflammation and M2 microglia: the good, the bad, and the inflamed. *J Neuroinflammation*. 11:98.
- Choi, J., D.R. Nordli, Jr., T.D. Alden, A. DiPatri, Jr., L. Laux, K. Kelley, J. Rosenow, S.U. Schuele, V. Rajaram, and S. Koh. 2009. Cellular injury and neuroinflammation in children with chronic intractable epilepsy. *J Neuroinflammation*. 6:38.
- Conrady, C.D., D.A. Drevets, and D.J.J. Carr. 2010. Herpes simplex type I (HSV-1) infection of the nervous system: Is an immune response a good thing? *Journal of Neuroimmunology*. 220:1-9.

- Cowan, L.D. 2002. The epidemiology of the epilepsies in children. *Mental Retardation and Developmental Disabilities Research Reviews*. 8:171-181.
- Culhane, A.C., M.D. Hall, N.J. Rothwell, and G.N. Luheshi. 1998. Cloning of rat brain interleukin-18 cDNA. *Molecular Psychiatry*. 3:362.
- Davies, K.G., B.P. Hermann, and A.R. Wyler. 1995. Surgery for intractable epilepsy secondary to viral encephalitis. *Br J Neurosurg*. 9:759-762.
- De Groot, C.J.A., E. Bergers, W. Kamphorst, R. Ravid, C.H. Polman, F. Barkhof, and P. van der Valk. 2001. Post-mortem MRI-guided sampling of multiple sclerosis brain lesions: Increased yield of active demyelinating and (p)reactive lesions. *Brain*. 124:1635-1645.
- de Jong, B.A., T.W.J. Huizinga, E.L.E.M. Bollen, B.M.J. Uitdehaag, G.P.T. Bosma, M.A. van Buchem, E.J. Remarque, A.C.S. Burgmans, N.F. Kalkers, C.H. Polman, and R.G.J. Westendorp. 2002. Production of IL-1 β and IL-1Ra as risk factors for susceptibility and progression of relapse-onset multiple sclerosis. *Journal of Neuroimmunology*. 126:172-179.
- de Rivero Vaccari, J.P., W.D. Dietrich, and R.W. Keane. 2014. Activation and regulation of cellular inflammasomes: gaps in our knowledge for central nervous system injury. *Journal of Cerebral Blood Flow & Metabolism*. 34:369-375.
- Dinarello, C.A. 1999. IL-18: A TH1 -inducing, proinflammatory cytokine and new member of the IL-1 family. *Journal of Allergy and Clinical Immunology*. 103:11-24.
- Dube, C.M., A.L. Brewster, C. Richichi, Q. Zha, and T.Z. Baram. 2007. Fever, febrile seizures and epilepsy. *Trends Neurosci*. 30:490-496.
- E. Vince, J., and J. Silke. 2016. The intersection of cell death and inflammasome activation.
- Edye, M., L. Walker, G. Sills, D. Brough, and S. Allan. 2014. Epilepsy and the inflammasome: Targeting inflammation as a novel therapeutic strategy for seizure disorders. 4 pp.
- Epstein, L.G., S. Shinnar, D.C. Hesdorffer, D.R. Nordli, A. Hamidullah, E.K. Benn, J.M. Pellock, L.M. Frank, D.V. Lewis, S.L. Moshe, R.C. Shinnar, and S. Sun. 2012. Human herpesvirus 6 and 7 in febrile status epilepticus: the FEBSTAT study. *Epilepsia*. 53:1481-1488.
- Felderhoff-Mueser, U., O. Schmidt, A. Oberholzer, C. Bühner, and P. Stahel. 2005. IL-18: A key player in neuroinflammation and neurodegeneration? 487-493 pp.
- French, J.A., P.D. Williamson, V.M. Thadani, T.M. Darcey, R.H. Mattson, S.S. Spencer, and D.D. Spencer. 1993. Characteristics of medial temporal lobe epilepsy: I. Results of history and physical examination. *Ann Neurol*. 34:774-780.
- Friedman, H., L. Ch'ien, and D. Parham. 1977. Virus in brain of child with hemiplegia, hemiconvulsions, and epilepsy. *Lancet*. 2:666.
- Gilbert, M.T.P., T. Haselkorn, M. Bunce, J.J. Sanchez, S.B. Lucas, L.D. Jewell, E.V. Marck, and M. Worobey. 2007. The Isolation of Nucleic Acids from Fixed, Paraffin-Embedded Tissues—Which Methods Are Useful When? *PLoS One*. 2:e537.
- Gloor, S.M., M. Wachtel, M.F. Bolliger, H. Ishihara, R. Landmann, and K. Frei. 2001. Molecular and cellular permeability control at the blood-brain barrier. *Brain Res Brain Res Rev*. 36:258-264.
- González-Navajas, J.M., J. Lee, M. David, and E. Raz. 2012. Immunomodulatory functions of type I interferons. *Nat Rev Immunol*. 12:125-135.
- Gross, O., C. Groß, G. Guarda, and J. Tschopp. 2011. The inflammasome: An integrated view. 136-151 pp.
- Haberland, C. 2006. *Clinical Neuropathology: Text and Color Atlas*. Springer Publishing Company.
- Hanamsagar, R., M.L. Hanke, and T. Kielian. 2012. Toll-like receptor (TLR) and Inflammasome Actions in the Central Nervous System: New and Emerging Concepts. *Trends in Immunology*. 33:333-342.
- Heneka, M.T., M.P. Kummer, and E. Latz. 2014. Innate immune activation in neurodegenerative disease. *Nat Rev Immunol*. 14:463-477.

- Huang, W.-X., P. Huang, and J. Hillert. 2004. Increased expression of caspase-1 and interleukin-18 in peripheral blood mononuclear cells in patients with multiple sclerosis. 482-487 pp.
- Imaizumi, T., S. Nishizaka, M. Ayabe, H. Shoji, T. Ichiyama, and Y. Sugita. 2005. Probable chronic viral encephalitis with microglial nodules in the entire brain: a case report with necropsy. *Med Sci Monit.* 11:CS23-26.
- James, S.H., D.W. Kimberlin, and R.J. Whitley. 2009. Antiviral Therapy for Herpesvirus Central Nervous System Infections: Neonatal Herpes Simplex Virus Infection, Herpes Simplex Encephalitis, and Congenital Cytomegalovirus Infection. *Antiviral research.* 83:207-213.
- Jander, S., and G. Stoll. 1998. Differential induction of interleukin-12, interleukin-18, and interleukin-1 β converting enzyme mRNA in experimental autoimmune encephalomyelitis of the Lewis rat. *Journal of Neuroimmunology.* 91:93-99.
- Jay, V., L.E. Becker, H. Otsubo, M. Cortez, P. Hwang, H.J. Hoffman, and M. Zielenska. 1995. Chronic encephalitis and epilepsy (Rasmussen's encephalitis): detection of cytomegalovirus and herpes simplex virus 1 by the polymerase chain reaction and in situ hybridization. *Neurology.* 45:108-117.
- Jha, S., S. Y Srivastava, J. Brickey, H. Iocca, A. Toews, J. Morrison, V. S Chen, D. Gris, G. K Matsushima, and J. P-Y Ting. 2010. The Inflammasome Sensor, NLRP3, Regulates CNS Inflammation and Demyelination via Caspase-1 and Interleukin-18. 15811-15820 pp.
- Jonas, R., S. Nguyen, B. Hu, R.F. Asarnow, C. LoPresti, S. Curtiss, S. de Bode, S. Yudovin, W.D. Shields, H.V. Vinters, and G.W. Mathern. 2004. Cerebral hemispherectomy: hospital course, seizure, developmental, language, and motor outcomes. *Neurology.* 62:1712-1721.
- Keller, M., A. Rüegg, S. Werner, and H.-D. Beer. 2008. Active Caspase-1 Is a Regulator of Unconventional Protein Secretion. *Cell.* 132:818-831.
- Khansari, N., Y. Shakiba, and M. Mahmoudi. 2009. Chronic inflammation and oxidative stress as a major cause of age-related diseases and cancer. *Recent Pat Inflamm Allergy Drug Discov.* 3:73-80.
- Kim, B.-H., J.D. Chee, C.J. Bradfield, E.-S. Park, P. Kumar, and J.D. MacMicking. 2016. IFN-induced Guanylate Binding Proteins in Inflammasome Activation and Host Defense. *Nature immunology.* 17:481-489.
- Kimberlin, D.W. 2007. Management of HSV encephalitis in adults and neonates: diagnosis, prognosis and treatment. *Herpes.* 14:11-16.
- Kleinschmidt-DeMasters, B.K., R.L. DeBiasi, and K.L. Tyler. 2001. Polymerase chain reaction as a diagnostic adjunct in herpesvirus infections of the nervous system. *Brain Pathol.* 11:452-464.
- Lamkanfi, M., and V.M. Dixit. 2009. The Inflammasomes. *PLoS Pathogens.* 5:e1000510.
- Lammerding, L., A. Slowik, S. Johann, C. Beyer, and A. Zendedel. 2016. Poststroke Inflammasome Expression and Regulation in the Peri-Infarct Area by Gonadal Steroids after Transient Focal Ischemia in the Rat Brain. *Neuroendocrinology.* 103:460-475.
- Laukoter, S., H. Rauschka, A.R. Tröscher, U. Köck, E. Saji, K. Jellinger, H. Lassmann, and J. Bauer. 2017. Differences in T cell cytotoxicity and cell death mechanisms between progressive multifocal leukoencephalopathy, herpes simplex virus encephalitis and cytomegalovirus encephalitis. *Acta Neuropathol.* 133:613-627.
- Lewis, D.V., S. Shinnar, D.C. Hesdorffer, E. Bagiella, J.A. Bello, S. Chan, Y. Xu, J. MacFall, W.A. Gomes, S.L. Moshe, G.W. Mathern, J.M. Pellock, D.R. Nordli, Jr., L.M. Frank, J. Provenzale, R.C. Shinnar, L.G. Epstein, D. Masur, C. Litherland, and S. Sun. 2014. Hippocampal sclerosis after febrile status epilepticus: the FEBSTAT study. *Ann Neurol.* 75:178-185.
- Lin, J., S.H. Kennedy, T. Svarovsky, J. Rogers, J.W. Kemnitz, A. Xu, and K.T. Zondervan. 2009. High-quality genomic DNA extraction from formalin-fixed and paraffin-embedded samples deparaffinized using mineral oil. *Analytical Biochemistry.* 395:265-267.

- Lu, M., X.-L. Sun, C. Qiao, Y. Liu, J.-H. Ding, and G. Hu. 2014. Uncoupling protein 2 deficiency aggravates astrocytic endoplasmic reticulum stress and nod-like receptor protein 3 inflammasome activation. *Neurobiology of Aging*. 35:421-430.
- Matin, N., O. Tabatabaie, R. Falsaperla, R. Lubrano, P. Pavone, F. Mahmood, M. Gullotta, A. Serra, P. Di Mauro, S. Cocuzza, and G. Vitaliti. 2015. Epilepsy and innate immune system: A possible immunogenic predisposition and related therapeutic implications. *Hum Vaccin Immunother*. 11:2021-2029.
- Meng, X.-F., L. Tan, M.-S. Tan, T. Jiang, C.-C. Tan, M.-M. Li, H.-F. Wang, and J.-T. Yu. 2014. Inhibition of the NLRP3 inflammasome provides neuroprotection in rats following amygdala kindling-induced status epilepticus. *J Neuroinflammation*. 11:212.
- Mori, I., M.J. Hossain, K. Takeda, H. Okamura, Y. Imai, S. Kohsaka, and Y. Kimura. 2001. Impaired Microglial Activation in the Brain of IL-18-Gene-Disrupted Mice after Neurovirulent Influenza A Virus Infection. *Virology*. 287:163-170.
- Nagyösz, P., Á. Nyúl-Tóth, C. Fazakas, I. Wilhelm, M. Kozma, J. Molnár, J. Haskó, and I.A. Krizbai. 2015. Regulation of NOD-like receptors and inflammasome activation in cerebral endothelial cells. *Journal of Neurochemistry*. 135:551-564.
- Nahmias, A.J., R.J. Whitley, A.N. Visintine, Y. Takei, and C.A. Alford, Jr. 1982. Herpes simplex virus encephalitis: laboratory evaluations and their diagnostic significance. *J Infect Dis*. 145:829-836.
- Nakahira, M., H.-J. Ahn, W.-R. Park, P. Gao, M. Tomura, C.-S. Park, T. Hamaoka, T. Ohta, M. Kurimoto, and H. Fujiwara. 2002. Synergy of IL-12 and IL-18 for IFN- γ Gene Expression: IL-12-Induced STAT4 Contributes to IFN- γ Promoter Activation by Up-Regulating the Binding Activity of IL-18-Induced Activator Protein 1. *The Journal of Immunology*. 168:1146.
- Nguyen, M.D., J.P. Julien, and S. Rivest. 2002. Innate immunity: the missing link in neuroprotection and neurodegeneration? *Nat Rev Neurosci*. 3:216-227.
- Okamura, H., H. Tsutsui, T. Komatsu, M. Yutsudo, A. Hakura, T. Tanimoto, K. Torigoe, T. Okura, Y. Nukada, K. Hattori, K. Akita, M. Namba, F. Tanabe, K. Konishi, S. Fukuda, and M. Kurimoto. 1995. Cloning of a new cytokine that induces IFN- γ production by T cells. *Nature*. 378:88.
- Olson, L.C., E.L.C. Buescher, M.S. Artenstein, and P.D. Parkman 1967. Herpesvirus Infections of the Human Central Nervous System. *New England Journal of Medicine*. 277:1271-1277.
- Ousman, S.S., and P. Kubes. 2012. Immune surveillance in the central nervous system. *Nat Neurosci*. 15:1096-1101.
- Owens, G.C., M.N. Huynh, J.W. Chang, D.L. McArthur, M.J. Hickey, H.V. Vinters, G.W. Mathern, and C.A. Kruse. 2013. Differential expression of interferon- γ and chemokine genes distinguishes Rasmussen encephalitis from cortical dysplasia and provides evidence for an early Th1 immune response. *J Neuroinflammation*. 10:56-56.
- Pardo, C.A., E.P. Vining, L. Guo, R.L. Skolasky, B.S. Carson, and J.M. Freeman. 2004. The pathology of Rasmussen syndrome: stages of cortical involvement and neuropathological studies in 45 hemispherectomies. *Epilepsia*. 45:516-526.
- Pavlovic, D., A.C. Patera, F. Nyberg, M. Gerber, M. Liu, and C. for the Progressive Multifocal Leukoencephalopathy. 2015. Progressive multifocal leukoencephalopathy: current treatment options and future perspectives. *Therapeutic Advances in Neurological Disorders*. 8:255-273.
- Perucca, E., J. French, and M. Bialer. 2007. Development of new antiepileptic drugs: challenges, incentives, and recent advances. *The Lancet Neurology*. 6:793-804.
- Pestka, S., C.D. Krause, and M.R. Walter. 2004. Interferons, interferon-like cytokines, and their receptors. *Immunological Reviews*. 202:8-32.
- Pitkanen, A., I. Kharatishvili, H. Karhunen, K. Lukasiuk, R. Immonen, J. Nairismagi, O. Grohn, and J. Nissinen. 2007. Epileptogenesis in experimental models. *Epilepsia*. 48 Suppl 2:13-20.
- Platanias, L.C., and E.N. Fish. 1999. Signaling pathways activated by interferons. *Experimental Hematology*. 27:1583-1592.

- Power, C., S.D. Poland, W.T. Blume, J.P. Girvin, and G.P. Rice. 1990. Cytomegalovirus and Rasmussen's encephalitis. *Lancet*. 336:1282-1284.
- Prayson, R.A. 2010. 23 - Pathology of Epilepsy A2 - Perry, Arie. In *Practical Surgical Neuropathology*. D.J. Brat, editor. Churchill Livingstone, New York. 515-526.
- Quinnan, G.V., Jr., H. Masur, A.H. Rook, G. Armstrong, W.R. Frederick, J. Epstein, J.F. Manischewitz, A.M. Macher, L. Jackson, J. Ames, and et al. 1984. Herpesvirus infections in the acquired immune deficiency syndrome. *Jama*. 252:72-77.
- Ramaswamy, V., J.G. Walsh, D.B. Sinclair, E. Johnson, R. Tang-Wai, B.M. Wheatley, W. Branton, F. Maingat, T. Snyder, D.W. Gross, and C. Power. 2013. Inflammasome induction in Rasmussen's encephalitis: cortical and associated white matter pathogenesis. *J Neuroinflammation*. 10:152.
- Rasmussen, T., J. Olszewski, and D. Lloydsmith. 1958. Focal seizures due to chronic localized encephalitis. *Neurology*. 8:435-445.
- Rauch, I., M. Müller, and T. Decker. 2013. The regulation of inflammation by interferons and their STATs. *JAK-STAT*. 2:e23820.
- Ravizza, T., B. Gagliardi, F. Noé, K. Boer, E. Aronica, and A. Vezzani. 2008. Innate and adaptive immunity during epileptogenesis and spontaneous seizures: Evidence from experimental models and human temporal lobe epilepsy. *Neurobiology of Disease*. 29:142-160.
- Rawlings, J.S., K.M. Rosler, and D.A. Harrison. 2004. The JAK/STAT signaling pathway. *Journal of Cell Science*. 117:1281.
- Richardson, E.P., Jr., and H.D. Webster. 1983. Progressive multifocal leukoencephalopathy: its pathological features. *Prog Clin Biol Res*. 105:191-203.
- Sayyah, M., M. Javad-Pour, and M. Ghazi-Khansari. 2003. The bacterial endotoxin lipopolysaccharide enhances seizure susceptibility in mice: involvement of proinflammatory factors: nitric oxide and prostaglandins. *Neuroscience*. 122:1073-1080.
- Scharfman, H.E. 2007. The Neurobiology of Epilepsy. *Current neurology and neuroscience reports*. 7:348-354.
- Schroder, K., and J. Tschopp. 2010. The Inflammasomes. *Cell*. 140:821-832.
- Shi, F.-D., K. Takeda, S. Akira, N. Sarvetnick, and H.-G. Ljunggren. 2000. IL-18 Directs Autoreactive T Cells and Promotes Autodestruction in the Central Nervous System Via Induction of IFN- γ by NK Cells. *The Journal of Immunology*. 165:3099.
- Singh, S., I. Metz, S. Amor, P. van der Valk, C. Stadelmann, and W. Brück. 2013. Microglial nodules in early multiple sclerosis white matter are associated with degenerating axons. *Acta Neuropathol*. 125:595-608.
- Song, L., L. Pei, S. Yao, Y. Wu, and Y. Shang. 2017. NLRP3 Inflammasome in Neurological Diseases, from Functions to Therapies. *Frontiers in Cellular Neuroscience*. 11:63.
- Steiner, I., H. Budka, A. Chaudhuri, M. Koskiniemi, K. Sainio, O. Salonen, and P.G. Kennedy. 2005. Viral encephalitis: a review of diagnostic methods and guidelines for management. *Eur J Neurol*. 12:331-343.
- Sutterwala, F.S., S. Haasken, and S.L. Cassel. 2014. Mechanism of NLRP3 inflammasome activation. *Annals of the New York Academy of Sciences*. 1319:82-95.
- Takei, H., A. Wilfong, A. Malphrus, D. Yoshor, J.V. Hunter, D.L. Armstrong, and M.B. Bhattacharjee. 2010. Dual pathology in Rasmussen's encephalitis: a study of seven cases and review of the literature. *Neuropathology*. 30:381-391.
- Thom, M. 2014. Review: Hippocampal sclerosis in epilepsy: a neuropathology review. *Neuropathol Appl Neurobiol*. 40:520-543.
- van de Veerdonk, F.L., M.G. Netea, C.A. Dinarello, and L.A.B. Joosten. 2011. Inflammasome activation and IL-1 β and IL-18 processing during infection. *Trends in Immunology*. 32:110-116.
- van den Pol, A.N. 2006. Viral infections in the developing and mature brain. *Trends Neurosci*. 29:398-406.
- van Noort, J.M., M. Bsibsi, W.H. Gerritsen, P. van der Valk, J.J. Bajramovic, L. Steinman, and S. Amor. 2010. α B-Crystallin Is a Target for Adaptive Immune Responses and a

- Trigger of Innate Responses in Preactive Multiple Sclerosis Lesions. *Journal of Neuropathology & Experimental Neurology*. 69:694-703.
- Varadkar, S., C.G. Bien, C.A. Kruse, F.E. Jensen, J. Bauer, C.A. Pardo, A. Vincent, G.W. Mathern, and J.H. Cross. 2014. Rasmussen's encephalitis: clinical features, pathobiology, and treatment advances. *Lancet Neurol*. 13:195-205.
- Varatharaj, A., and I. Galea. 2017. The blood-brain barrier in systemic inflammation. *Brain Behav Immun*. 60:1-12.
- Vespa, P.M., D.L. McArthur, Y. Xu, M. Eliseo, M. Etchepare, I. Dinov, J. Alger, T.P. Glenn, and D. Hovda. 2010. Nonconvulsive seizures after traumatic brain injury are associated with hippocampal atrophy. *Neurology*. 75:792-798.
- Vezzani, A., J. French, T. Bartfai, and T.Z. Baram. 2011. The role of inflammation in epilepsy. *Nat Rev Neurol*. 7:31-40.
- Vezzani, A., and T. Granata. 2005. Brain Inflammation in Epilepsy: Experimental and Clinical Evidence. *Epilepsia*. 46:1724-1743.
- Walker, M.C. 2015. Hippocampal Sclerosis: Causes and Prevention. *Semin Neurol*. 35:193-200.
- Walter, G.F., and R.R. Renella. 1989. Epstein-Barr virus in brain and Rasmussen's encephalitis. *Lancet*. 1:279-280.
- Weissert, R. 2011. Progressive multifocal leukoencephalopathy. *Journal of Neuroimmunology*. 231:73-77.
- White, C.S., C.B. Lawrence, D. Brough, and J. Rivers-Auty. 2017. Inflammasomes as therapeutic targets for Alzheimer's disease. *Brain Pathol*. 27:223-234.
- Whitley, R.J., S.J. Soong, C. Linneman, Jr., C. Liu, G. Pazin, and C.A. Alford. 1982. Herpes simplex encephalitis. Clinical Assessment. *Jama*. 247:317-320.
- Wuthrich, C., S. Kesari, W.K. Kim, K. Williams, R. Gelman, D. Elmeric, U. De Girolami, J.T. Joseph, T. Hedley-Whyte, and I.J. Koralnik. 2006. Characterization of lymphocytic infiltrates in progressive multifocal leukoencephalopathy: co-localization of CD8(+) T cells with JCV-infected glial cells. *J Neurovirol*. 12:116-128.
- Zhou, K., L. Shi, Y. Wang, S. Chen, and J. Zhang. 2016. Recent Advances of the NLRP3 Inflammasome in Central Nervous System Disorders. *Journal of Immunology Research*. 2016:9238290.

7 Appendix

7.1 Clinical data of included patients

Sample number	Disease	Stage of Disease	Male/Female	Hemisphere	Sample Area	Autopsy/Surgery
91/10/4	Healthy Control	-	m	r	Gyrus cinguli right	Autopsy
140/05/1	Healthy Control	-	m	l	Frontal left	Autopsy
395/99/f	Epileptic Control	-	m	l	Temporal cortex	Epilepsy surgery
35/10/10	Epileptic Control	-	m	r	Temporal cortex	Epilepsy surgery
1181/11/7	Epileptic Control	-	m	l	Temporal cortex	Epilepsy surgery
826/06/b	Epileptic Control	-	m	l	Temporal cortex	Epilepsy surgery
1998/05/12	Epileptic Control	-	f	l	Temporal cortex	Epilepsy surgery
723/10/5	Epileptic Control	-	f	l	Temporal cortex	Epilepsy surgery
805/11/I3	Epileptic Control	-	f	l	Temporal cortex	Epilepsy surgery
764/10/II3	Epileptic Control	-	f	l	Temporal cortex	Epilepsy surgery
143/12/II2	RE	0	f	l	Cortex Hemispherotomy	Epilepsy surgery
Y304/12/13	RE	0	m	l	Cortex Hemispherectomy	Epilepsy surgery
221/02/e	RE	0	m	r	Temporal cortex	Epilepsy surgery
128/14/I3	RE	0	f		Temporal cortex	Epilepsy surgery
247/05/II2	RE	0 & 1	m	r	Temporal cortex	Epilepsy surgery
57/03/I6	RE	0	f	l	Cortex Hemispherotomy	Epilepsy surgery
834/03/a4	RE	0	m	r	Temporal cortex	Epilepsy surgery
144/14	RE	1	m	r	Temporal cortex	Epilepsy surgery
1065/96/12	RE	1	m	l	Hippocampus	Epilepsy surgery
912/93/I7	RE	1	f	l	Temporal cortex	Epilepsy surgery
1762/00/14(I)	RE	1	f	r	Frontal cortex	Epilepsy surgery
1471/97	RE	1	m	unknown	unknown	Epilepsy surgery
877/12/II2	RE	1 & 2	m	r	Insula	Epilepsy surgery
201/15/II2	RE	1.5	f	l	Cortex Hemispherotomy	Epilepsy surgery
899/13/II2	RE	2	f	r	Temporal cortex	Epilepsy surgery
542/12/IIb	RE	2	f	l	Cortex Hemispherotomy	Epilepsy surgery
127/15/I	RE	2	m	r	Amygdala	Epilepsy surgery
61/14/II2	RE	2	m	r	Cortex Hemispherotomy	Epilepsy surgery
1909/96/15	RE	2	m	r	Frontal cortex	Epilepsy surgery
247/05/I8	RE	2	m	r	Temporal cortex	Epilepsy surgery
57/03/I3	RE	3	f	l	Cortex Hemispherotomy	Epilepsy surgery
1166/91/III1,4	RE	3	f	r	Cortex Hemispherotomy	Epilepsy surgery
1414/91/8b	RE	3	f	l	Frontal cortex	Epilepsy surgery
441/09/I	MTLE	-	m	l	Hippocampus	Epilepsy surgery
209/15/IV1	MTLE	-	m	r	Hippocampus	Epilepsy surgery

218/15/IV1	MTLE	-	f	r	Hippocampus	Epilepsy surgery
234/15/IV1	MTLE	-	m	r	Hippocampus	Epilepsy surgery
141/15/III1	MTLE	-	m	l	Hippocampus	Epilepsy surgery
149/15/III1	MTLE	-	m	r	Hippocampus	Epilepsy surgery
174/15/IV1	MTLE	-	m	l	Hippocampus	Epilepsy surgery
1519/99/b2	MTLE + Enc	-	f	r	Hippocampus	Epilepsy surgery
1006/09/d	MTLE + Enc	-	m	l	Hippocampus	Epilepsy surgery
741/10/b	MTLE + Enc	-	m	r	Hippocampus	Epilepsy surgery
1578/04/5	MTLE + Enc	-	m	l	Hippocampus	Epilepsy surgery
364/92/4	CMV	-	m	-	-	Autopsy
455/92/4	CMV	-	m	-	-	Autopsy
234/93/4	CMV	-	m	-	-	Autopsy
118/94/2	CMV	-	m	-	-	Autopsy
430/93/6	CMV	-	m	-	-	Autopsy
559/92/11	CMV	-	m	-	-	Autopsy
62/94/9	CMV	-	m	-	-	Autopsy
97/93/1	PML	-	m	-	-	Autopsy
496/85/6	PML	-	m	-	-	Autopsy
359/93/10	PML	-	m	-	-	Autopsy
47/83/3	PML	-	m	-	-	Autopsy
278/93/6	PML	-	unknown	-	-	Autopsy
214/98*/5	PML	-	m	-	-	Autopsy
514/82/10	HSV	-	m	-	-	Autopsy
67/83/2	HSV	-	f	-	-	Autopsy
204/83/4	HSV	-	m	-	-	Autopsy
285/82/1	TBE	-	f	-	-	Autopsy
266/84/1	TBE	-	f	-	-	Autopsy
295/84/1	TBE	-	m	-	-	Autopsy
460/84/3	TBE	-	m	-	-	Autopsy
245/90/3	TBE	-	m	-	-	Autopsy

Table 1. Clinical data of included patients.